LuxT controls specific quorum-sensing-regulated behaviors in *Vibrionaceae* spp. via repression of *qrr*1, encoding a small regulatory RNA

LuxT represses the quorum-sensing sRNA, Qrr1

Michaela J. Eickhoff[1], Chenyi Fei[1,2], Xiuliang Huang[1,3], and Bonnie L. Bassler[1,3]*

[1]Department of Molecular Biology, Princeton University, Princeton, New Jersey, USA.

[2]Lewis-Sigler Institute for Integrative Genomics, Princeton University, Princeton, New Jersey, USA.

[3]Howard Hughes Medical Institute, Chevy Chase, MD 20815, USA.

*Corresponding author
Email: bbassler@princeton.edu

Abstract

Quorum sensing (QS) is a process of chemical communication bacteria use to transition between individual and collective behaviors. QS depends on the production, release, and synchronous response to signaling molecules called autoinducers (AIs). The marine bacterium *Vibrio harveyi* monitors AIs using a signal transduction pathway that relies on five small regulatory RNAs (called Qrr1-5) that post-transcriptionally control target genes. Curiously, the small RNAs largely function redundantly making it difficult to understand the necessity for five of them. Here, we identify LuxT as a transcriptional repressor of *qrr*1. LuxT does not regulate *qrr*2-5, demonstrating that *qrr* genes can be independently controlled to drive unique downstream QS gene expression patterns. LuxT reinforces its control over the same genes it regulates indirectly via repression of *qrr*1, through a second transcriptional control mechanism. Genes dually regulated by LuxT specify public goods including an aerolysin-type pore-forming toxin. Phylogenetic analyses reveal that LuxT is conserved among *Vibrionaceae* and sequence comparisons predict that LuxT represses *qrr*1 in additional species. The present findings reveal that the QS regulatory RNAs can carry out both shared and unique functions to endow bacteria with plasticity in their output behaviors.

Author Summary

Bacteria communicate and count their cell numbers using a process called quorum sensing (QS). In response to changes in cell density, QS bacteria alternate between acting as individuals and participating in collective behaviors. *Vibrio harveyi* is used as a

model organism to understand QS-mediated communication. Five small RNAs lie at the heart of the *V. harveyi* QS system, and they regulate the target genes that underlie the QS response. The small RNAs largely function redundantly making it difficult to understand why *V. harveyi* requires five of them. Here, we discover a regulator, called LuxT, that exclusively represses the gene encoding one of the QS small RNAs. LuxT regulation of one QS small RNA enables unique control of a specific subset of QS target genes. LuxT is broadly conserved among *Vibrionaceae*. Our findings show how redundant regulatory components can possess both common and unique roles that provide bacteria with plasticity in their behaviors.

Introduction

Bacteria can coordinate gene expression on a population-wide scale using a process of cell-cell communication called quorum sensing (QS). QS depends on the production, release, and detection of signal molecules called autoinducers (AIs). Because AIs are self-produced by the bacteria, as cell density increases, extracellular AI levels likewise increase. Bacteria respond to accumulated AIs by collectively altering gene expression, and in turn, behavior. QS-regulated processes include bioluminescence, biofilm formation, and the secretion of virulence factors [1,2].

Vibrio harveyi is a model marine bacterium that uses QS to regulate over 600 genes [3-8]. *V. harveyi* produces and responds to three AIs, which act in parallel. The LuxM synthase produces AI-1 (*N*-(3-hydroxybutanoyl)-L-homoserine), LuxS produces AI-2 ((2*S*,4*S*)-2-methyl-2,3,3,4-tetrahydroxytetrahydrofuran-borate), and CqsA produces

89 CAI-1 ((*Z*)-3-aminoundec-2-en-4-one)) [3,9-16]. The three AIs are recognized by the
90 cognate receptors LuxN, LuxPQ, and CqsS, respectively [13,14,17]. At low cell density
91 (LCD, Fig 1A), when little AI is present, the unbound receptors act as kinases that transfer
92 phosphate to the phosphorelay protein LuxU, which shuttles the phosphoryl group to the
93 response regulator, LuxO [4,6,18,19]. LuxO-P, together with the alternative sigma factor
94 σ^{54}, activates expression of genes encoding five non-coding small regulatory RNAs
95 (sRNAs), Qrr1-5, that function post-transcriptionally [6,20,21]. The five Qrr sRNAs
96 promote translation of *aphA* and repress translation of *luxR,* encoding the LCD and high
97 cell density (HCD) QS master transcriptional regulators, respectively (Fig 1A) [20,22-27].
98 When the Qrr sRNAs are produced, individual behaviors are undertaken and the
99 luciferase operon (*luxCDABE*), responsible for the canonical bioluminescence QS output
100 in *V. harveyi,* is not expressed. At HCD (Fig 1B), when the AIs bind to their cognate
101 receptors, the receptors' kinase activities are inhibited, allowing their phosphatase
102 activities to dominate. Consequently, phospho-flow through the QS circuit is reversed
103 [28]. Dephosphorylated LuxO is inactive. Thus, Qrr1-5 are not produced, *aphA* translation
104 is not activated, and *luxR* translation is not repressed (Fig 1B). In this state, LuxR is
105 produced, and it controls expression of genes underpinning group behaviors. Notably,
106 LuxR activates expression of *luxCDABE*, causing *V. harveyi* cells to make light at HCD
107 [14].

108 The five *V. harveyi* Qrr sRNAs have high sequence identity and they are predicted
109 to possess similar secondary structures with four stem loops [20]. Mechanistic studies of
110 Qrr3 as the exemplar Qrr showed it regulates translation of its different target mRNAs by

four mechanisms, all mediated by the chaperone Hfq; repression via catalytic degradation of the mRNA target, repression via coupled degradation of Qrr3 with the mRNA target, repression through sequestration of the mRNA target, and activation via revelation of the mRNA ribosome-binding site [26]. In addition to *aphA* and *luxR,* the Qrr sRNAs also feedback to repress *luxO* and *luxMN* translation [29,30]. Microarray analyses following *qrr* overexpression revealed 16 additional Qrr-controlled target mRNAs [31].

The extreme relatedness of the Qrr sRNAs, coupled with their similar QS-controlled production patterns, has made it difficult to assign any unique role to a particular Qrr sRNA. Nonetheless, among the Qrr sRNAs, Qrr1 stands out: it lacks nine nucleotides in stem loop 1 that are present in Qrr2-5 [20,27,31]. Due to this difference, Qrr1 does not regulate *aphA* and two of the other known target mRNAs [31]. Qrr2-5 regulate an identical set of target mRNAs [31]. Thus, the failure of Qrr1 to control one subset of mRNAs is the only functional difference known among the Qrr sRNAs. Also of note is the position of *qrr*1 in the *V. harveyi* genome: *qrr*1 is located immediately upstream of *luxO*, oriented in the opposite direction [20,21]. No other *qrr* genes reside near known QS genes.

Predicted LuxO-P and σ^{54} binding sites lie upstream of each *qrr* gene. The sites vary in sequence and relative position with respect to the *qrr* transcriptional start sites. Other than these sites, there is little sequence similarity between *qrr* promoter regions [20,21]. There also exist hallmarks of transcription factor binding sites upstream of *qrr* genes, which differ in every case, hinting that unique factors could regulate each *qrr* gene [20]. Indeed, while all the Qrr sRNAs are made at LCD, they exhibit distinct production

profiles. Specifically, in order of highest to lowest expression: Qrr4 > Qrr2 > Qrr3 > Qrr1 > Qrr5 [20]. The strength by which each Qrr sRNA represses *luxR* translation, and therefore downstream bioluminescence emission, correlates with Qrr production level: Qrr4 is the strongest repressor of light production, while Qrr1 and Qrr5 are the weakest [19,20]. When introduced into *Escherichia coli*, all five *qrr* sRNA genes are activated to high levels by LuxO D61E, a LuxO-P mimetic, suggesting that regulation by additional factors, that are not present in *E. coli*, occurs in *V. harveyi* [20]. Investigating the possibility that other regulators are involved in *qrr* control *in vivo* is the subject of the present work.

LuxT is a 17 kDa transcriptional regulator of the AcrR/TetR family, initially identified as a protein that binds strongly to DNA containing the region upstream of the *V. harveyi luxO* gene [32,33]. An approximate 50 bp region that is bound by LuxT was discovered [32]. A follow-up report showed that LuxT activates light production in *V. harveyi*, the presumption being that LuxT functioned via repression of *luxO* [33]. At the time of this earlier study, the Qrr sRNAs had not been discovered and LuxO was assumed to be a repressor of bioluminescence. Thus, the logic of the first LuxT manuscripts were: LuxT represses *luxO,* and LuxO represses luciferase.

Research undertaken since the original LuxT publications has led to the current understanding of mechanisms underlying *V. harveyi* QS-controlled gene regulation (Fig 1). Key is that LuxO phosphorylation, not *luxO* expression, is regulated (Fig 1). This incongruity inspired us to reconsider the earlier findings concerning LuxT. Here, we explore the role of LuxT in *V. harveyi* QS with a focus on its connection to *qrr*1. We show

that LuxT does indeed bind upstream of *luxO* at the site originally identified [32]. However, LuxT does not regulate *luxO*. While the experiments in the initial manuscripts were rigorously performed and interpreted appropriately, the authors could not have known that the gene encoding Qrr1 is located adjacent to *luxO*. We discover that the LuxT binding region is located within the *qrr*1 promoter. Indeed, we show that LuxT represses the transcription of *qrr*1 at LCD. LuxT does not repress *qrr*2-5. Relative to wild-type (WT) *V. harveyi*, in a Δ*luxT* mutant, *qrr*1 is expressed more highly at LCD. As a consequence, Qrr1 is available to post-transcriptionally regulate its target genes, including a gene encoding an extracellular protease (*VIBHAR_RS11785*), a gene encoding a pore-forming aerolysin toxin (*VIBHAR_RS11620*), a gene encoding a chitin deacetylase (*VIBHAR_RS16980*), and a gene specifying a component involved in capsular polysaccharide secretion (*VIBHAR_RS25670*) [31]. In addition to indirect activation of these genes via repression of *qrr*1, LuxT also activates transcription of these same four genes. Finally, we show that LuxT repression of *qrr*1 transcription is not specific to *V. harveyi.* LuxT also represses *qrr*1 in *Aliivibrio fischeri,* a species that, interestingly, harbors only a single Qrr sRNA: *qrr*1. Phylogenetic analyses show that *luxT* is conserved among *Vibrionaceae* and suggest that LuxT may repress *qrr*1 in other species within the *Vibrionaceae* family. Together, our results support a new QS model that incorporates LuxT and provides a mechanism for the unique control of one of the Qrr sRNA genes, *qrr*1. This newly revealed regulatory arrangement shows how Qrr1 controls downstream targets distinct from those controlled by the other Qrr sRNAs.

Results

LuxT binds upstream of *luxO* but does not repress *luxO* transcription

In the original works that identified and studied *V. harveyi* LuxT, DNA binding assays revealed the LuxT binding site to be a roughly 50 bp region lying 76 bp upstream of the *luxO* start codon [32]. (We note that in those reports, the site was designated to be 117 bp upstream of *luxO*, due to initial mis-annotation of the *luxO* start codon.) By assaying changes in light production, the authors concluded that LuxT represses *luxO* transcription [33]. This result is curious because our subsequent work showed that *luxO* is transcribed constitutively and only its phosphorylation state changes in response to QS signaling [19,34]. Indeed, all fluctuations in LuxO levels in *V. harveyi* have been ascribed to intrinsic noise [34]. To confirm that LuxT binds upstream of *luxO,* we conducted electrophoretic mobility shift assays (EMSAs) using purified LuxT protein. Analogous to the results described by Lin et al. [32], LuxT caused a shift of a 95 bp DNA probe encompassing the *luxO* promoter region, whereas no significant binding to a control DNA probe occurred (Fig 2A). In the context of the 95 bp *luxO* promoter probe, randomizing the DNA sequence of the identified 50 bp LuxT binding region nearly eliminated LuxT binding (S1 Fig). Also consistent with the initial findings, deletion of *luxT* caused an ~11-fold reduction in light production by *V. harveyi* at LCD, indicating that LuxT is a LCD activator of luciferase (Fig 2B) [33]. At HCD (OD_{600} > 1), the WT and Δ*luxT V. harveyi* strains exhibited similar light

198 production profiles (Fig 2B). Therefore, LuxT activation of luciferase expression is cell-
199 density dependent, indicating a possible role for QS.

200 The implication from the above findings, based on the original work, is that LuxT
201 functions via repression of *luxO*. To investigate this possibility, we measured *luxO*
202 transcript levels in WT and Δ*luxT V. harveyi*. We also measured transcript levels of *luxC,*
203 the first gene in the luciferase operon. There were no detectable differences in *luxO*
204 transcript levels in the WT and Δ*luxT* strains at either LCD or HCD (Fig 2C and 2D,
205 respectively). Thus, LuxT does not repress *luxO* transcription. By contrast, and consistent
206 with the results in Fig 2B, WT *V. harveyi* possessed 7-fold more *luxC* mRNA than did
207 Δ*luxT V. harveyi* at LCD (Fig 2C) while the difference was only 2-fold at HCD (Fig 2D).
208 Thus, LuxT activates *luxCDABE* expression, primarily at LCD. Finally, measurements of
209 AphA and LuxR protein levels showed no significant differences between the WT and
210 Δ*luxT* strains at either LCD or HCD (Fig 2E). Because *aphA* and *luxR* lie downstream of
211 LuxO in the QS circuit, changes in LuxO levels necessarily drive changes in AphA and
212 LuxR levels, albeit in opposite directions (Fig 1 and [8,24,29]). We conclude that LuxT
213 has no role in regulating *luxO* expression. Therefore, LuxT activation of light production
214 must occur through an alternative mechanism. We return to this point below.

215

216 **LuxT represses *qrr*1, not *luxO*, transcription**

217

218 As mentioned in the Introduction, at the time of the Lin *et al.* studies, the Qrr sRNAs that
219 function between LuxO and QS target genes had not been discovered. Thus, Lin *et al.*

could not have known that *qrr*1 lies immediately upstream and in the opposite orientation of *luxO* in the *V. harveyi* genome. In fact, *qrr*1 is located in closer proximity to the identified LuxT binding region than *luxO*. Specifically, if +1 designates the *qrr*1 transcriptional start site, the LuxT DNA binding region spans bases -76 to -27, suggesting that LuxT binds in the *qrr*1 promoter between the predicted LuxO-P and σ^{54} binding sites that are essential for activation of *qrr*1 transcription (Fig 3A and S2 Fig) [20,21,32].

To test our prediction that LuxT represses *qrr*1 transcription, not *luxO* transcription, we employed two fluorescent reporters. First, we constructed a *qrr*1 promoter fusion containing the 193 nucleotides immediately upstream of *qrr*1 fused to *mRuby3.* Thus, the promoter fragment harbored the LuxO-P, LuxT, and σ^{54} binding sites. A consensus ribosome-binding site was included to drive *mRuby3* translation. Second, a *luxO* promoter fusion was constructed by cloning the same 193 bp DNA fragment in the opposite orientation upstream of *mRuby3.* Reporter fluorescence was measured in four *V. harveyi* strains: WT, *luxO* D61E, Δ*luxT,* and *luxO* D61E Δ*luxT.* As mentioned, *V. harveyi luxO* D61E encodes a LuxO-P mimetic. LuxO D61E constitutively activates *qrr*1-5, causing strains harboring this mutant allele to display a “LCD-locked” phenotype irrespective of the actual culture cell density [19]. The *V. harveyi luxO* D61E strain is a crucial tool for our studies. It enables investigation of the consequences of maximal *qrr* transcription when the culture cell density is high enough to allow accurate measurements of QS-controlled gene expression using reporter assays or qRT-PCR [20,21]. The output of the P_{qrr1}-*mRuby3* reporter was low in the WT, *luxO* D61E, and Δ*luxT V. harveyi* strains (Fig 3B). This result was expected because *qrr*1 exhibits only low-level expression in *V.*

242 *harveyi,* even at LCD [20]. Eight-fold higher expression of P_{qrr1}-*mRuby3* occurred in the
243 *luxO* D61E Δ*luxT V. harveyi* strain (Fig 3B). Regarding the P_{luxO}-*mRuby3* reporter,
244 compared to the WT, the output was lower in the *V. harveyi* strains harboring *luxO* D61E
245 (Fig 3C). This result was also expected because a negative feedback loop exists between
246 LuxO-P and *luxO* [29]. What is crucial is that elimination of *luxT* caused no change in
247 P_{luxO}-*mRuby3* reporter expression compared to WT and caused no further change in the
248 *luxO* D61E mutant (Fig 3C). Together, the *qrr*1 and *luxO* reporters show that LuxT does
249 not regulate *luxO.* Rather, LuxT represses *qrr*1 transcription.
250 The distinct level of *in vivo* expression displayed by each *qrr* gene in *V. harveyi*
251 has been interpreted to suggest that, beyond being controlled by LuxO-P, each *qrr* gene
252 is controlled independently by other regulators [20]. Figure 3B shows that LuxT is one
253 such regulator of *qrr*1. To investigate whether LuxT also regulates *qrr*2-5, levels of all five
254 Qrr sRNAs were measured using qRT-PCR in WT, Δ*luxT, luxO* D61E, and *luxO* D61E
255 Δ*luxT V. harveyi* strains. Confirming the reporter assay results, Qrr1 levels were ~4 fold
256 higher in the *luxO* D61E Δ*luxT* strain than in the other three strains (Fig 3D). While
257 increased levels of Qrr2-5 were detected in the *luxO* D61E strain compared to WT,
258 deletion of *luxT* did not cause any additional changes (Fig 3D). Verification of the qRT-
259 PCR results comes from analyses of *mRuby3* transcriptional reporters to *qrr*2-5. All four
260 reporters displayed higher activity in the *luxO* D61E *V. harveyi* strain than in WT, and
261 deletion of *luxT* had no effect (S3 Fig). Therefore, among the *qrr* genes, LuxT exclusively
262 represses *qrr*1.
263

LuxT activates *luxCDABE* via a mechanism that is independent of Qrr1

Our next goal was to investigate how LuxT activates expression of *luxCDABE*, given that the mechanism is not via repression of *luxO*. The Qrr sRNAs repress *luxR* translation, and therefore they indirectly repress *luxCDABE* (Fig 1). Thus, an obvious possibility is that LuxT repression of *qrr*1 activates luciferase. However, *luxR* is downstream of Qrr1 (Fig 1) and Fig 2E shows that deletion of *luxT* does not significantly alter LuxR levels at LCD, suggesting that LuxT does not control luciferase via a LuxR-dependent mechanism. To validate this finding, we tested whether Qrr1 is required for LuxT to activate light production. To do this, we measured bioluminescence from a *V. harveyi* Δ*luxT* mutant and compared it to that made by a Δ*luxT* Δ*qrr*1 double mutant. Both strains exhibited the identical phenotype: ~10-fold reduced light production relative to WT *V. harveyi* and the Δ*qrr*1 mutant (S4 Fig). Thus, LuxT activation of luciferase occurs by a mechanism that is independent of Qrr1.

We next tested the possibility that LuxT directly activates *luxCDABE* transcription. The *luxCDABE* promoter and regulatory region extend approximately 350 bp upstream of the *luxC* start codon [35-37]. To determine if LuxT binds within this region, we amplified six overlapping DNA fragments from -405 to +81 relative to the *luxC* start codon (S5A Fig). Compared to the avid binding of LuxT to the *qrr*1 promoter (Fig 2A), LuxT bound the *luxC* promoter only very weakly. Specifically, binding to all the *luxC* promoter-containing DNA fragments was comparable to the binding of LuxT to control (*E. coli lacZ)* DNA (Fig 2A and S5B-D Fig) with modestly stronger binding to Probe 3 (S5C Fig). As another test

for direct LuxT activation of luciferase, we introduced plasmid-borne arabinose-inducible *luxT* and a plasmid with IPTG-inducible *luxR* into recombinant *E. coli* carrying *luxCDABE*. LuxR is a direct activator of *luxCDABE* [22,37,38]. As expected, induction of *luxR* drove increased light production compared to the empty vector control (S6A Fig). By contrast, induction of *luxT* did not increase light production in the presence or absence of *luxR* (S6A Fig). We confirmed that *luxT* was expressed from the plasmid using qRT-PCR (S6B Fig). We note that induction of *luxT* expression in *E. coli* caused a modest growth defect (S6C Fig). In conclusion, we find no evidence that LuxT directly activates *luxCDABE.*

To further investigate the mechanism underlying LuxT activation of luciferase, we probed whether LuxT functions via other known QS components. To do this, we compared the bioluminescence profiles of the *V. harveyi* Δ*qrr*1-5, Δ*luxO*, and *luxO* D61E strains to the identical strains lacking *luxT* (S7A-C Fig). We also included a test of the *VIBHAR_RS03920* gene (S7D Fig), a homolog of *Vibrio parahaemolyticus swrZ.* In *V. parahaemolyticus,* SwrT, the LuxT equivalent, represses *swrZ* encoding a GntR family transcription factor, which in turn, represses lateral flagellar (*laf*) genes [39]. We considered that in *V. harveyi*, LuxT could repress *VIBHAR_RS03920*, which could repress *luxCDABE*. In all four cases, introduction of the *luxT* deletion reduced light output (S7A-D Fig). Thus, LuxT activates *luxCDABE* by a mechanism that does not require *qrr*1-5*, luxO,* or *VIBHAR_RS03920*. We could not perform a similar experiment to assess whether LuxT regulation of *luxCDABE* is LuxR-dependent because the Δ*luxR* mutant makes no light. However, as mentioned above, LuxR protein levels are similar in WT and Δ*luxT V. harveyi* (Fig 2E), and moreover, there are no significant differences in *luxR* or

aphA transcript levels between WT and Δ*luxT V. harveyi* at LCD (S8 Fig). Thus, LuxT affecting *luxCDABE* expression via regulation of *luxR* does not seem a reasonable possibility. To conclude, unfortunately, we did not discover the mechanism by which LuxT activates luciferase. We do know that the mechanism is likely indirect and that the component that connects LuxT to *luxCDABE* is not any of the regulators in the *V. harveyi* QS pathway. From here forward, we focus on the consequences of LuxT regulation of *qrr*1. In future studies, we hope to define the mechanism by which LuxT activates light production.

LuxT controls target genes via repression of *qrr*1

Only low-level expression of *qrr*1 occurs in WT *V. harveyi*, including at LCD, and that feature has made it difficult to detect Qrr1-mediated regulatory effects *in vivo*. Based on our discovery of LuxT repression of *qrr*1, we hypothesize that LuxT activity could mask Qrr1 function *in vivo*. If so, LuxT would indirectly activate the known Qrr1-repressed mRNA targets. To test this possibility, we used qRT-PCR to compare the levels of Qrr1 mRNA targets in *V. harveyi luxO* D61E to that in *V. harveyi luxO* D61E Δ*luxT*. We assayed the 14 Qrr1 target genes that lie outside the QS pathway [31] as well as *luxR* and *luxMN*, Qrr1 targets that function inside the QS system [20,27,30]. Deletion of *luxT* caused a significant decrease in the mRNA levels of 9 of the 16 tested genes (S9A Fig). Thus, we suspected that LuxT activated expression of the 9 genes via repression of *qrr*1. To test this prediction, we compared transcript levels of the 9 genes in *V. harveyi luxO* D61E, *V.*

330 *harveyi luxO* D61E Δ*qrr*1, *V. harveyi luxO* D61E Δ*luxT*, and *V. harveyi luxO* D61E Δ*qrr*1
331 Δ*luxT*. To our surprise, in all cases, the two strains lacking *luxT* possessed lower levels
332 of the transcripts than did the two strains possessing *luxT* (S9B Fig). These data show
333 that these target genes are controlled by LuxT in a Qrr1-independent manner.
334 The data in S9B Fig inspired us to expand our LuxT/Qrr1 regulatory model to
335 include two key findings: (1) LuxT represses *qrr*1, encoding a sRNA that post-
336 transcriptionally regulates target genes (Fig 3 and [31]), and (2) LuxT also activates
337 expression of the same target genes, independently of Qrr1. Thus, we propose that LuxT
338 functions by two mechanisms to activate expression of the 9 target genes, one
339 transcriptionally and one post-transcriptionally: LuxT is a transcriptional activator of the
340 target genes and LuxT additionally activates the target genes by repressing their
341 repressor, Qrr1.
342 To test the above model, we focused on the four most highly LuxT-regulated target
343 genes: *VIBHAR_RS11785, VIBHAR_RS11620, VIBHAR_RS16980,* and
344 *VIBHAR_RS25670.* First, to examine whether LuxT indeed activates their transcription,
345 we eliminated Qrr-dependent regulation using a *V. harveyi* Δ*qrr*1-5 strain. In all four
346 cases, transcript levels were lower in the Δ*qrr*1-5 Δ*luxT* strain than in the Δ*qrr*1-5 strain.
347 Complementation with *luxT* expressed from a plasmid restored the transcript levels,
348 confirming that LuxT activates the expression of these genes via a Qrr-independent
349 mechanism (Fig 4A). To demonstrate that LuxT control of these genes is exerted at the
350 level of transcription, we made *lux* transcriptional reporters and measured their outputs in
351 *luxA*::Tn*5* and *luxA*::Tn*5* Δ*luxT V. harveyi* strains. Using a *luxA* null mutant for this

352 analysis ensured that all light production came from the transcriptional fusions. All four
353 reporters exhibited lower activity in the *luxA*::Tn*5* Δ*luxT* strain than in the *luxA*::Tn*5* strain
354 (~400, 4, 48, and 7-fold lower activity for, respectively, *VIBHAR_RS11785,*
355 *VIBHAR_RS11620, VIBHAR_RS16980,* and *VIBHAR_RS25670*, S10 Fig). These data
356 confirm an aspect of our model: LuxT activates transcription of these target genes.
357 The second tenet of our model, that LuxT activates expression of the target genes
358 via repression of *qrr*1 cannot be detected by the above qRT-PCR assay (S9B Fig). Figure
359 4B-C depicts the issue. In WT *V. harveyi*, transcription of *qrr*1 is repressed by LuxT.
360 Therefore, deletion of *qrr*1 has no effect on target gene regulation (Fig 4B and S9B Fig).
361 In Δ*luxT V. harveyi*, *qrr*1 expression is de-repressed. However, in the absence of the
362 LuxT activator, transcription of the target genes does not occur. Thus, although Qrr1 is
363 present, its mRNA targets are absent, so again regulation via Qrr1 does not occur (Fig
364 4C).
365 To circumvent these issues and probe the connection of LuxT to Qrr1 in post-
366 transcriptional regulation of the four target genes, we used a strategy in which we
367 eliminated LuxT transcriptional control of the target genes to unmask post-transcriptional
368 effects. To accomplish this, we constructed translational fusions to the fluorescent protein
369 mVenus. DNA upstream of each target gene containing the site that base pairs with Qrr1
370 and the ribosome-binding site was cloned in frame with *mVenus* downstream of the
371 tetracycline-inducible *tetA* promoter. Therefore, the fusions were constitutively
372 transcribed following addition of aTc, irrespective of the presence or absence of *luxT*.
373 Analogously designed translational reporters were previously shown to be repressed in

374 *E. coli* following *qrr*1 overexpression [31]. We confirmed that the reporters are all activated
375 by aTc and repressed following overexpression of *qrr*1 in *V. harveyi* (S11 Fig).

376 The translational mVenus reporter fusions were used to test the second aspect of
377 our model in which we predict that LuxT activates target genes post-transcriptionally via
378 *qrr*1 repression. Reporter activities from the four target gene constructs were measured
379 in the following LCD-locked *V. harveyi* strains: *luxO* D61E, *luxO* D61E Δ*luxT, luxO* D61E
380 Δ*qrr*1, and *luxO* D61E Δ*qrr*1 Δ*luxT*. The results for all four reporters were similar (Fig 5A-
381 D). The *luxO* D61E strain exhibited higher reporter activity than the *luxO* D61E Δ*luxT*
382 strain, presumably due to the de-repression of *qrr*1 that occurs in the absence of LuxT.
383 Importantly, deletion of *luxT* in the *luxO* D61E Δ*qrr*1 strain had no effect on reporter
384 translation (Fig 5A-D, compare *luxO* D61E Δ*qrr*1 and *luxO* D61E Δ*qrr*1 Δ*luxT* bars). We
385 conclude that LuxT post-transcriptionally regulates the four tested genes in a Qrr1-
386 dependent manner. We note that higher translation of the reporters occurred in the *luxO*
387 D61E Δ*qrr*1 strains than the *luxO* D61E strains containing *qrr*1 (Fig 5A-D). This pattern is
388 consistent with Qrr1 functioning as a repressor, and we interpret the result to mean that
389 when the *qrr*1 gene is present, residual Qrr1 production occurs, including in the presence
390 of LuxT. We presume that this pattern cannot be observed in the qRT-PCR analyses (S9B
391 Fig) because Qrr1 represses translation of target genes by a sequestration mechanism
392 that does not significantly alter mRNA levels [26, 31].

393 The four genes that are regulated transcriptionally by LuxT and post-
394 transcriptionally by LuxT via Qrr1 encode a peptidase (*VIBHAR_RS11785*), an aerolysin
395 toxin (*VIBHAR_RS11620*), a chitin disaccharide deacetylase (*VIBHAR_RS16980*), and a

protein involved in export of capsular polysaccharide (*VIBHAR_RS25670*). Interestingly, all four genes are secreted public goods or involved in secretion of public goods (i.e., *VIBHAR_RS25670*), a class of components that are commonly controlled by QS. We focus on the aerolysin toxin (*VIBHAR_RS11620*) here to probe *in vivo* LuxT and Qrr1 regulation. Secreted aerolysin-like toxins form pores in eukaryotic cells, and in the case of red blood cells, cause lysis [40]. Thus, aerolysin hemolytic activity can be assessed by growing bacteria on blood agar plates and monitoring them for zones of clearance. We used this assay to test if LuxT and Qrr1 influence aerolysin secretion according to our dual-mechanism model (Fig 4B). First, the *V. harveyi luxO* D61E strain exhibited modest clearing, whereas no clearing occurred around the *luxO* D61E Δ*luxT* strain (Fig 5E). This result is consistent with LuxT functioning as an activator of aerolysin production. Second, compared to the *luxO* D61E strain, *luxO* D61E Δ*qrr*1 showed increased hemolytic activity (Fig 5E). This result can be explained by Qrr1-mediated post-transcriptional repression of *VIBHAR_RS11620* (Fig 5B). Finally, the *luxO* D61E Δ*qrr*1 Δ*luxT* strain did not display hemolytic activity (Fig 5E). In agreement with our model (Fig 4B,C), the transcriptional effect of LuxT overrides the post-transcriptional effect of Qrr1. The hemolysis activities of the identical strains were also quantified using a liquid assay (S12 Fig). Analogous results were obtained for the four strains, except that the *luxO* D61E strain exhibited a level of hemolytic activity similar to that of the *luxO* D61E Δ*qrr*1 strain. Possibly, this discrepancy is due to the different growth conditions used for the plate and liquid hemolysis assays.

LuxT represses *qrr*1 in *A. fischeri*

In members of the *Vibrionaceae* family, AI structures and the types of proteins employed as receptors vary between species. However, LuxO is conserved in all sequenced vibrio species [41] and LuxT is also often present [39,42-44] and we address this further in the next section. We wondered whether LuxT-mediated repression of *qrr*1 is *V. harveyi* specific or whether LuxT has this function in other *Vibrionaceae* species. To explore this question, we tested three species, *Vibrio cholerae, V. parahaemolyticus,* and *A. fischeri* in experiments analogous to those in Fig 3B. Plasmids harboring transcriptional reporter fusions to *qrr*1 from each representative species were introduced into WT, Δ*luxT, luxO* D61E, and *luxO* D61E Δ*luxT* strains of those species. As mentioned, *luxT* is called *swrT* in *V. parahaemolyticus*, and the LCD-locked LuxO-P mimetic in *A. fischeri* is *luxO* D55E. In *V. cholerae,* LuxO D61E activated the P_{qrr1}-*luxCDABE* reporter relative to WT, however elimination of *luxT* did not affect reporter activity in either strain (S13A Fig). Activity from the *V. parahaemolyticus* P_{qrr1}-*mRuby3* reporter remained low in all four strains (S13B Fig). Thus, we do not find evidence for *qrr*1 repression by LuxT in *V. cholerae* or by SwrT *V. parahaemolyticus.* We note, however, that regarding *V. parahaemolyticus*, we cannot rule out the presence of an additional *qrr*1 repressor that masks LuxT function and maintains *qrr*1 transcription at an especially low level.

A. fischeri is distantly related to *V. harveyi* and, curiously, *A. fischeri* only encodes a single *qrr* gene, *qrr*1, and Qrr1 post-transcriptionally represses LitR, the LuxR homolog (Fig 6A) [45]. Through additional regulatory steps, activation of LitR drives the downstream activation of *luxCDABE* [46]. The *A. fischeri* P_{qrr1}-*mRuby3* reporter exhibited

low-level expression in the WT, Δ*luxT,* and *luxO* D55E strains (Fig 6B). However higher fluorescence was emitted in the *A. fischeri luxO* D55E Δ*luxT* strain (Fig 6B). Thus, as in *V. harveyi,* LuxT is a repressor of *qrr*1 in *A. fischeri.*

The redundancy among the five Qrr sRNAs in *V. harveyi* prevents the elimination of *qrr*1 from driving large effects on LuxR levels (Fig 2E and [20]), and in the context of the present work, masks the consequences of deletion of *luxT*. Because no Qrr redundancy exists in *A. fischeri,* we predicted that LuxT repression of *qrr*1 would affect LitR levels. Indeed, compared to the *A. fischeri luxO* D55E strain, the *luxO* D55E Δ*luxT* strain showed a 4-fold reduction in *litR* transcript levels (Fig 6C). To test if this manifestation of LuxT occurs via repression of *qrr*1, we measured *litR* transcription in *A. fischeri luxO* D55E Δ*qrr*1 and *A. fischeri luxO* D55E Δ*qrr*1 Δ*luxT*. There was no significant difference in *litR* transcript levels showing that LuxT activates *litR* expression in a Qrr1-dependent manner (Fig 6C). The differences in *litR* transcript levels observed between the *luxO* D55E and *luxO* D55E Δ*qrr*1 strains are likely a result of Qrr1 feedback control of *luxO* [29]. To determine if the observed LuxT-dependent effects on LitR likewise affect downstream expression of luciferase, we measured bioluminescence in the four *A. fischeri* strains. Indeed, the *luxO* D55E Δ*luxT* strain made less light than the *luxO* D55E strain (Fig 6D). The *luxO* D55E Δ*qrr*1 and *luxO* D55E Δ*qrr*1 Δ*luxT* strains emitted similar levels of light showing that LuxT controls light production in *A. fischeri* via regulation of *qrr*1 (Fig 6D). We conclude that LuxT is a repressor of *qrr*1 in *A. fischeri*, and because Qrr1 is the sole Qrr, LuxT has a more major role in controlling the overall QS state in *A.*

fischeri than in *V. harveyi.* We discuss possible advantages of the different regulatory arrangements below.

Putative LuxT regulation of *qrr*1 is diversified in the *Vibrionaceae* family

Members of the *Vibrionaceae* family can be divided into two classes, those encoding a single *qrr* upstream of *luxO,* and those encoding multiple *qrr* loci [21,45]. Species with multiple *qrr* genes always encode *qrr*1 upstream of *luxO,* suggesting that *qrr*1 is the ancestral gene. Our finding of LuxT repression of *qrr*1 in both *V. harveyi* and *A. fischeri* inspired us to investigate whether LuxT is conserved among all *Vibrionaceae* family members, and if so, whether LuxT possesses an evolutionary pattern that corresponds to that of the Qrr sRNAs. To compare *luxT* and *qrr* phylogenies, we scanned all *Vibrionaceae* sequenced genomes to identify *qrr* genes, expanding on previous analyses [21]. The majority of species within the *Vibrio* genus encoded multiple *qrr* loci, most often 4 or 5 *qrr* genes, like *V. cholerae* and *V. harveyi*, respectively (Fig 7A). All members of non-*Vibrio* genera encoded only a single *qrr* gene, like *A. fischeri*, except for *Photobacterium galatheae*, which had no putative *qrr* gene (Fig 7A). Analogous examination of the genomes for *luxT* homologs showed that *luxT* genes exist in most *Vibrionaceae* species possessing one and multiple *qrr* genes (Fig 7B). Within the *Vibrio* genus, species lacking apparent *qrr* genes also lacked *luxT* homologs, and the *luxT* genes were more similar to *V. harveyi luxT* in species with multiple *qrr* genes than were the *luxT* genes in species possessing only a single *qrr* gene.

To predict whether LuxT does or does not control *qrr*1 expression in a particular species, we compared the DNA sequences upstream of *qrr*1 in the four *Vibrionaceae* species tested in our experiments. The σ^{54} binding sites are highly conserved among the four species (Fig 7C and [20,21]), while the LuxT binding regions show less conservation. Thus, harboring a *luxT* homolog does not necessarily signify that it controls *qrr*1. The "GGTTAAA" upstream of *qrr*1 in the LuxT binding region was the most conserved sequence between the species. Consistent with our experimental results, the *V. cholerae* sequence in this region, i.e., "GATTTG–", is the most dissimilar from those of the other three species (Fig 7C). This sequence divergence may underlie our finding that LuxT does not regulate *qrr*1 in *V. cholerae* (S13 Fig). In *V. parahaemolyticus*, this region is identical to that in *V. harveyi*. However, we do not observe LuxT regulation of *qrr*1 in *V. parahaemolyticus* (S13 Fig). As mentioned above, *qrr*1 expression in *V. parahaemolyticus* may be too low to detect repression by LuxT, possibly due to additional repression by another factor. To more broadly examine the conservation of LuxT binding regions, we also performed phylogenetic analysis comparing the putative LuxT binding regions in the *qrr*1 promoters of all *Vibrionaceae* family members possessing both *qrr*1 and *luxT* genes. A variety of sequences exist (Fig 7D), and we find no evidence for a correlation between the number of *qrr* genes and similarity in the upstream LuxT binding regions. It remains possible that the DNA binding domains of LuxT coevolve with the DNA sequences in the LuxT binding regions. Together, our results indicate that while *qrr*1 and *luxT* are broadly conserved in *Vibrionaceae* species, LuxT regulation of *qrr*1 has diversified. Going forward, we will combine experimental and bioinformatic approaches

505 to pinpoint the precise LuxT binding site, determine its conservation between species,
506 and define the ramifications of particular DNA sequence changes.
507
508 **Discussion**
509
510 To survive, bacteria must appropriately respond to fluctuating environments. For marine
511 bacteria such as *V. harveyi,* successfully competing against a diversity of other microbes
512 and adapting to dynamic microscale nutrient gradients are key [47,48]. Sensory relays
513 that tune gene expression via transcriptional and post-transcriptional mechanisms enable
514 bacteria to overcome varying environmental challenges [49]. In the context of the present
515 work, QS signal transduction allows bacteria to monitor their changing cell numbers and
516 transition between executing individual and collective activities [50].
517 In vibrios, one or more Qrr sRNAs function at the core of QS signaling pathways,
518 and thus the concentration of Qrr sRNAs present at any time dictates the QS output
519 response in which hundreds of genes are either activated or repressed. The Qrr sRNAs,
520 and other bacterial sRNAs, are post-transcriptional regulators. Bacterial sRNAs are
521 thought to be especially beneficial regulators due to the low metabolic cost of their
522 production coupled with their fast synthesis and turnover rates, the latter of which can
523 drive rapid changes in target mRNA levels [51,52]. Moreover, because the QS Qrr sRNAs
524 function by multiple mechanisms (sequestration, catalytic mRNA degradation, coupled
525 mRNA-sRNA degradation, and mRNA translational activation), they can confer distinct
526 timing and expression levels to particular target genes providing “bespoke” QS output

527 responses [26]. These features of sRNAs are presumed to drive dynamic patterns of gene
528 expression that might not be achievable through the use of canonical transcription factors.
529 Gene duplication has led to the *V. harveyi* QS circuit harboring five similar Qrr
530 sRNAs [20]. Beyond QS, in bacteria it is common for multiple sRNAs to function
531 redundantly in a single pathway. Presumably, possessing more than one copy of a sRNA
532 gene can increase the available sRNA pool, and in turn, confer increased control over
533 target gene expression. In addition or alternatively, duplication may allow individual sRNA
534 genes to diversify, in sequence and/or in expression pattern, either or both of which can
535 enable differential regulatory effects [53]. Indeed, regarding the *V. harveyi* Qrr sRNAs,
536 deletion analyses and Qrr quantitation studies have demonstrated that the pool of Qrr
537 sRNAs available to regulate downstream target gene expression increases with
538 increasing numbers of *qrr* genes. Curiously, however, at least in the laboratory and with
539 *luxR* as the measured target gene, only four of the five Qrr sRNA genes are required to
540 achieve this effect. Thus, the final *qrr* duplication event does not appear to enhance
541 regulatory control [20]. Moreover, only low-level production of Qrr1 and Qrr5 have been
542 documented, suggesting that those two sRNAs do not contribute dramatically to changes
543 in the levels of the sRNA pool [20]. These findings, together with the knowledge that the
544 *qrr* promoter regions vary, has led us to hypothesize that some or all of the *qrr* genes may
545 be subject to additional control by as yet undefined regulatory components.
546 Here, our discovery of *V. harveyi* LuxT as a repressor of *qrr*1 provides evidence
547 for a QS model in which individual *qrr* genes are uniquely regulated. While LuxT
548 repression of *qrr*1 does not affect expression of the genes encoding the master QS

549 regulators LuxR and AphA, it does alter expression of a subset of Qrr1 target genes.
550 Separate from its role as a *qrr*1 repressor, we also found that LuxT controls the same set
551 of Qrr1 target genes at the transcriptional level. A regulatory strategy in which control is
552 exerted at two levels, via a transcriptional regulator and a post-transcriptional sRNA,
553 occurs in other systems and is proposed to prevent leaky target gene expression and to
554 alter target gene expression dynamics [54,55]. In the case of LuxT, at least four genes
555 are subject to such control, and they encode a protease, an aerolysin toxin, a chitin
556 deacetylase, and a gene involved in capsular polysaccharide secretion. Notably, all four
557 gene products are secreted, perhaps emphasizing the need for especially tight control of
558 public goods production. We imagine that LuxT initially evolved to transcriptionally
559 activate this set of target genes and later incorporated repression of *V. harveyi qrr*1 to
560 reinforce activation at the post-transcriptional level. Thus, the gene duplication events that
561 generated *qrr* redundancy in *V. harveyi* also provided the required substrate for regulation
562 by LuxT, ultimately enabling finely tuned expression of select members of the QS regulon
563 that rely on Qrr1, while avoiding blanket alteration of the QS response. Our discovery of
564 LuxT repression of *V. harveyi qrr*1 hints that analogous regulators may exist that uniquely
565 control *qrr*2-5.

566 The *luxT* gene is conserved among *Vibrionaceae* bacteria, but we only observe
567 LuxT repression of *qrr*1 in two of four tested species, *V. harveyi* and *A. fischeri*. These
568 two species harbor five and one *qrr* genes, respectively. More broadly, our phylogenetic
569 analyses of the LuxT binding regions upstream of *Vibrionaceae qrr*1 genes show that this
570 DNA sequence has diversified, and consistent with our results, may signify that LuxT

571 represses only a subset of *qrr*1 genes. Further investigation is necessary to understand
572 the regulatory logic underlying LuxT repression of *qrr*1 in some species but not in others.
573 We can speculate on these different circuit arrangements. To do so, we consider the
574 diversity of QS system components and regulatory architectures present in *Vibrionaceae*
575 species. We know from our and previous phylogenetic analyses that *luxO* is highly
576 conserved in vibrios, and species commonly possess from one to five *qrr* genes
577 [21,41,45,56]. Beyond these two core components, *Vibrionaceae* QS systems vary with
578 respect to the number and structures of QS AIs, the number, subcellular locations, and
579 signal relay mechanisms of the QS receptors, and the number and identities of the
580 downstream target genes [1,57,58]. Presumably, the differences in QS system
581 architectures represent the outcomes of distinct selective pressures experienced by
582 particular species over evolutionary time. As species diverged, a common set of parts
583 were mixed and matched, duplicated, and their placements in the regulatory hierarchies
584 altered with LuxO and the Qrr sRNAs remaining as the core of the QS networks. Similar,
585 but not identical QS systems emerged, each presumably capable of promoting ideal
586 biology for a given species. With regard to the present work, LuxT represents one more
587 component that evolution can insert into *Vibrionaceae* QS systems in different places in
588 the various hierarchies to enable it to specialize for each species.

589 Lastly, LuxT is a member of the bacterial TetR family of transcriptional regulators,
590 a widely distributed family of proteins possessing characteristic helix-turn-helix DNA-
591 binding domain [59]. *V. harveyi* LuxR is a member of this same protein family. Prior to our
592 discovery of *V. harveyi* LuxT as a *qrr*1 repressor, the functions of some LuxT homologs

had been studied including in *V. parahaemolyticus, A. fischeri, Vibrio vulnificus,* and *Vibrio alginolyticus.* In *V. parahaemolyticus*, the LuxT homolog, SwrT, activates genes promoting lateral-flagellar-driven swarming, enabling translocation across surfaces [39,60-62]. LuxT is a transcriptional activator of siderophore biosynthetic genes in *A. fischeri* [44]. In *V. vulnificus* and *V. alginolyticus,* LuxT is reported to control QS via regulation of expression of the *luxR* homologs [42,43]. Additionally, the *V. alginolyticus* Δ*luxT* mutant is defective for virulence in a zebrafish infection model [43]. Whether Qrr1 acts as a LuxT-controlled intermediary in these other vibrio pathways has not been investigated. These earlier studies, together with our findings that LuxT also controls gene expression independent of Qrr1 in *V. harveyi* hint that LuxT is a global regulator of gene expression in *Vibrionaceae*. Future transcriptomic analyses will be used to identify the set of genes comprising the *V. harveyi* LuxT regulon and to fully define which LuxT target genes are Qrr1 dependent and which are Qrr1 independent. Similar analyses in other *Vibrionaceae* species could reveal which functions of LuxT are general and which are species specific. Finally, it will be of particular interest to investigate the environmental signals that control *luxT* expression and LuxT activity. Under standard laboratory conditions, we have not observed variation in *luxT* mRNA or protein levels, however, examining its activity under conditions that more closely mimic nature may reveal how *luxT* itself is regulated.

Materials and Methods

Bacterial strains and culture conditions

V. harveyi strains were derived from *V. harveyi* BB120 (BAA-1116) [63]. *A. fischeri* strains were derivatives of *A. fischeri* ES114 [64]. *V. cholerae* strains were derived from *V. cholerae* C6706str2 [65], and *V. parahaemolyticus* strains were derived from *V. parahaemolyticus* BB22OP (LM5312) [66]. *E. coli* BW25113 was used for heterologous gene expression and *E. coli* S17 -1 λ*pir* was used for cloning. All strains are listed in Table S1. *Vibrio* and *Aliivibrio* strains were grown at 30°C shaking in either Luria Marine (LM) medium or minimal Autoinducer Bioassay (AB) medium, the latter supplemented with 0.4% vitamin-free casamino acids (Difco) [4,67]. *E. coli* strains were grown shaking at 37°C or at 30°C in LB medium. Antibiotics were added as follows (μg mL^{-1}): ampicillin, 100; chloramphenicol, 10; kanamycin, 100; polymyxin B, 50; and tetracycline, 10. Induction of genes on plasmids was accomplished by the addition of 0.5 mM isopropyl β-D-1-thiogalactopyranoside (IPTG) (Thermo Fisher), 0.2% arabinose (Sigma), or 100 ng mL^{-1} anhydrotetracycline (aTc) (Takara), as necessary.

DNA manipulation and strain construction

PCR reactions were carried out with either KOD Hot Start DNA Polymerase (Sigma) or iProof DNA Polymerase (Bio-Rad). Oligonucleotides were purchased at Integrated DNA Technologies (IDT) and are listed in S2 Table. A DNA fragment containing the randomized LuxT binding region was synthesized by IDT. Cloning was performed using

637 isothermal DNA assembly with the Gibson Assembly Master Mix (New England Biolabs)
638 [68]. All plasmids were validated by sequencing (Genewiz) and are listed in S3 Table.
639 Plasmids that enable overexpression of genes are designated with a lowercase p (e.g.
640 p*qrr*1). For reporter fusion constructs, a capital P designates the promoter that drives
641 transcription (e.g. P_{qrr1}-*mRuby3*). Transcriptional reporters to *luxO* and to *qrr*1 included
642 approximately 200 bp of promoter DNA upstream of *mRuby3*. Transcriptional reporters
643 to *qrr*2-5, *VIBHAR_RS11785, VIBHAR_RS11620, VIBHAR_RS16980,* and
644 *VIBHAR_RS25670* contained approximately 300 bp of promoter DNA. A consensus
645 ribosome binding site was included to drive translation. The putative base pairing regions
646 between Qrr1 and the *VIBHAR_RS11785, VIBHAR_RS11620,* and *VIBHAR_RS25670*
647 mRNAs were excluded from those reporter constructs. Due to its location far upstream of
648 the gene, the putative Qrr1 base pairing region for *VIBHAR_RS16980* could not be
649 excluded [31]. Translational reporters employing *mVenus* were designed using a
650 previously described method and transcribed from the aTc inducible *tetA* promoter
651 [31,69]. Plasmids were introduced into *E. coli* by electroporation using a Bio-Rad Micro
652 Pulser. Plasmids were introduced into *Vibrio* and *Aliivibrio* strains via conjugation with *E.*
653 *coli* S17-1 λ*pir. V. harveyi, V. cholerae,* and *V. parahaemolyticus* exconjugants were
654 selected on agar plates with polymyxin B. *A. fischeri* exconjugants were selected on agar
655 plates containing ampicillin. Chromosomal alterations in *Vibrio* and *Aliivibrio* strains were
656 generated using the pRE112 suicide vector harboring the *sacB* counter-selectable marker
657 as previously described [35,44,70]. Selection for the second crossover event was

performed on LM agar plates containing 15% sucrose (Sigma). Mutations were validated by PCR and/or sequencing.

LuxT-6xHis protein production and purification

The DNA encoding LuxT-6xHis was cloned into the pET-15b vector and the protein was overexpressed in *E. coli* BL21 (DE3) using 0.4 mM IPTG at 18°C for overnight growth. Cells were pelleted at 16,100 x *g* for 10 min and resuspended in lysis buffer (25 mM Tris-HCl pH 8, 150 mM NaCl) supplemented with 1 mM DTT, 2 mM PMSF, and 5 µM DNase I. The cells were lysed using sonication and subjected to centrifugation at 32,000 x *g* for 1 h. The LuxT-6xHis protein was purified from the clarified supernatant by Ni-NTA Superflow resin (Qiagen). Following washes with lysis buffer containing 20 mM Imidazole, the protein was eluted using lysis buffer containing 300 mM Imidazole. The collected elution fraction was loaded onto a HiTrap Q column (GE Healthcare) and further purified using a linear gradient of buffer A (25 mM Tris-HCl pH 8, 1 mM DTT) to buffer B (25 mM Tris-HCl pH 8, 1 M NaCl, 1 mM DTT). Peak fractions were pooled, concentrated, and subjected to a Superdex-200 size exclusion column (GE Healthcare) in gel filtration buffer (25 mM Tris-HCl pH 8, 100 mM NaCl, 1 mM DTT). The protein was concentrated, flash frozen, and stored at -80°C.

Electrophoretic mobility shift assays (EMSAs)

Oligonucleotide primers used to amplify DNA probes are listed in S2 Table. Reaction mixtures of 10 µL volume containing 20 nM dsDNA probe and 1:2 serial dilutions of LuxT-6xHis in low salt buffer (25 mM Tris pH 8, 50 mM NaCl) were incubated at room temperature for 15 min. LuxT-6xHis dimer concentrations ranged from 10 nM (0.5x) to 320 nM (16x). After incubation, 2.5 µL of 5X loading buffer (LightShift EMSA Optimization and Control Kit, Thermo) was added to the mixtures, and the samples were loaded onto a 6% Novex TBE DNA retardation gel (Thermo) at 4°C. Gels were subjected to electrophoresis in 1x TBE buffer at 100 V for 1.75 h. Gels were stained using SYBR Green I Nucleic Acid Gel Stain (Thermo) for 30 min. After five washes with 20 mL 1x TBE, gels were imaged using an ImageQuant LAS 4000 imager under the SYBR Green setting.

Bioluminescence assays

Cells from overnight cultures of *V. harveyi* were pelleted by centrifugation at 21,100 x *g* (Eppendorf 5424) and resuspended in fresh LM medium. Flasks containing 25 mL of LM medium were inoculated with the washed cells, normalizing each culture to a starting OD_{600} = 0.005. Culture flasks were incubated with shaking at 30°C. Every 45 min, bioluminescence and OD_{600} were measured using a Tri-Carb 2810 TR scintillation counter and DU800 spectrophotometer, respectively. *A. fischeri* cultures were grown as described for *V. harveyi* and bioluminescence was measured using a Tri-Carb 2810 TR scintillation counter when the OD_{600} = 1. To assay regulation of *luxCDABE* by LuxT*, E. coli* BW25113 harboring three plasmids, described in the legend to S6 Fig, was grown in

LB medium for 16 h at 30°C. Cells from cultures were pelleted by centrifugation at 21,100 x *g* (Eppendorf 5424) and resuspended in PBS. Bioluminescence and OD_{600} were measured as above. RNA was harvested as described below for qRT-PCR analysis of *luxT* overexpression. Transcriptional output from *VIBHAR_RS11785, VIBHAR_RS11620, VIBHAR_RS16980,* and *VIBHAR_RS25670 lux* fusions was measured from *V. harveyi* strains grown to OD_{600} = 1 in LM medium using a Tri-Carb 2810 TR scintillation counter. P_{qrr1}-*luxCDABE* activity was measured in *V. cholerae* strains using a BioTek Synergy Neo2 Multi-Mode Reader (BioTek, Winooski, VT, USA).

Quantitative real-time PCR analyses

Cells from overnight cultures of *V. harveyi* or *A. fischeri* were pelleted by centrifugation at 21,100 x *g* (Eppendorf 5424) and the cells were resuspended in fresh LM medium. 25 mL LM medium was inoculated with the washed cells, normalizing each culture to a starting OD_{600} = 0.005. The cultures were grown shaking at 30°C. At the desired cell densities, RNA was harvested from three independent cultures using the RNeasy mini kit (Qiagen #74106). RNA levels were normalized to 200 ng/µL and the samples were treated in two sequential reactions with DNase (Turbo DNA-free Kit, Thermo Fisher AM1907). cDNA was generated from 1 µg of RNA using Superscript III Reverse Transcriptase (Thermo Fisher, 18080093) as previously described [20]. Real-time PCR was performed using a QuantStudio 6 Flex Real-Time PCR detection system (Thermo Fisher) and PerfeCTa SYBR Green FastMix (Quantabio, 95074) as previously described [20]. In every case, 10

µL reactions were analyzed in quadruplicate technical replicates. Control reactions were performed with samples lacking reverse transcriptase and with samples lacking cDNA templates. Relative transcript levels were measured and normalized to an internal *hfq* control gene using a comparative $\Delta\Delta C_T$ method. qRT-PCR primers are listed in S2 Table.

Western blot analyses

Overnight cultures of WT and Δ*luxT V. harveyi* strains harboring either *aphA-3xFLAG* or *3xFLAG-luxR* at their native loci were pelleted by centrifugation at 21,100 x *g* (Eppendorf 5424) and resuspended in fresh LM medium. Flasks containing 125 mL LM medium were inoculated with the washed cells, normalizing the starting OD_{600} of each culture to 0.00001. When the cultures reached the desired cell densities, cells equivalent to 1 OD_{600} were pelleted by centrifugation at 2,808 x *g* for 10 min (Eppendorf 5810 R) and the pellets were flash frozen. Next, cells were lysed by resuspension in 150 µL of buffer containing 1x BugBuster (Sigma), 1x Halt Protease Inhibitors (Thermo Fisher), 0.5% Triton X-100 (Sigma), and 50 µg/mL lysozyme (Sigma). After incubation at room temperature for 30 min, proteins were solubilized in 1x SDS-PAGE buffer for 1 h at 37°C. Samples were loaded onto 4-20% TGX Stain-Free gels (Bio-Rad, #17000435) and subjected to electrophoresis at 50 mA for 30 min. Total loaded protein in the Stain-Free gel was visualized using an ImageQuant LAS 4000 imager using the EtBr setting. A second Stain-free gel was used for Western blot and was loaded with total protein levels normalized according to band intensities on the first gel. The normalization was verified by imaging.

A dominant band from this gel image serves as a loading control in Fig 2E. FLAG-tagged protein detection was performed as previously reported [71] using an Anti-FLAG M2-Peroxidase (HRP) antibody (Sigma, A8592) and bands were visualized using an ImageQuant LAS 4000 imager.

Fluorescence reporter assays

Fluorescent reporter plasmids are listed in S3 Table. The primers used to construct them are listed in S2 Table. Cells in overnight cultures of *Vibrio* or *Aliivibrio* strains harboring transcriptional or translational fluorescent reporter plasmids were pelleted by centrifugation at 21,100 x *g* (Eppendorf 5424) and washed in AB medium. AB medium was inoculated with the washed cells, normalizing each to OD_{600} = 0.005. 150 µL of the cultures were transferred to clear-bottom 96-well plates (Corning) in quadruplicate technical replicates. 50 µL of mineral oil was added to each well to prevent evaporation. The plates were shaken at 30°C, and fluorescence and OD_{600} were monitored over a 24 h period using a BioTek Synergy Neo2 Multi-Mode Reader. Relative fluorescence values represent the values when the OD_{600} reached 0.3 or 0.6, as indicated in the figure legends, for each sample. The OD_{600} values are the cell densities at which maximal differences between experimental and control reporter outputs could be measured.

Hemolysis assays

768 Cells in overnight cultures of *V. harveyi* were pelleted by centrifugation at 21,100 x *g*
769 (Eppendorf 5424) and resuspended in fresh LM medium. Culture densities were
770 normalized to OD_{600} = 1, and 2 µL of each culture were spotted onto a TSA plate
771 containing 5% sheep's blood (Thermo Fisher, R060312). The plates were incubated at
772 30°C for 72 h and imaged above a white light. To measure hemolysis activity in liquid
773 cultures, *V. harveyi* strains were grown for 24 h in AB medium. Cells were pelleted by
774 centrifugation at 21,100 x *g* (Eppendorf 5424), and the clarified culture fluids were filtered
775 through 0.22 µm filters (Sigma, SLGP033RB). Hemolysis of defibrinated sheep's blood
776 cells (Thomas Scientific, DSB030) was measured as previously described [72,73]. Briefly,
777 mixtures containing 1% blood cells in PBS and 25% of the filtered fluids were incubated
778 for 2 h at 37°C in in a 96-well plate. 1% blood cells were incubated in ddH_2O or PBS as
779 the positive and negative control, respectively. Following incubation, the plate was
780 subjected to centrifugation at 1,000 x *g* (Eppendorf 5810 R) for 5 min at 4°C, and 100 µL
781 of the resulting supernatants were transferred to a clean 96-well plate. Absorbance at 415
782 nm, indicative of blood cell lysis, was measured using a BioTek Synergy Neo2 Multi-Mode
783 Reader.
784
785 **Bioinformatic Analyses**
786
787 Genomic DNA sequences of 418 *Vibrionaceae* family members were downloaded from
788 the GenBank database (ftp.ncbi.nlm.nih.gov/genomes/genbank/bacteria/) [74]. To
789 identify genes encoding *qrr* or *luxT*, the chromosomes were scanned for regions similar

790 to the template sequences of *qrr* or *luxT*. As the query for *qrr* genes, we used the 3'-most
791 31 nucleotides of *V. harveyi qrr*1, which are highly homologous among all the *qrr* genes
792 in *V. harveyi*, *V. cholerae*, *A. fischeri*, and *V. parahaemolyticus* [20,21,27]. The DNA
793 encoding the entire *V. harveyi luxT* gene was used as the probe to identify other *luxT*
794 genes. Local sequence alignments were performed in MATLAB (Mathworks, 2020) using
795 the Smith-Waterman (SW) algorithm [75]. The standard scoring matrix NUC44 (see
796 ftp.ncbi.nih.gov/blast/matrices/) was used to compute similarity scores, which take into
797 account both the length and sequence similarity of the alignment. Cut-off values for the
798 similarity scores yielded from the SW algorithm were set to 30 for *qrr* genes and 100 for
799 *luxT* genes. Genes identified as possible *luxT* homologs were verified to encode TetR
800 family transcriptional regulators. Species lacking either *qrr*1 or *luxT* were excluded from
801 further phylogenetic analyses.
802
803 Multiple sequence alignments were performed using T-Coffee [76]. Phylogenetic
804 analyses and tree building were performed in MATLAB. To construct the phylogenetic
805 tree based on the putative LuxT binding regions residing upstream of *qrr*1 genes (see Fig
806 7), using the maximum-likelihood based Jukes-Cantor model [77], we first computed the
807 pairwise difference scores between the 30 nucleotides upstream of the σ^{54} binding sites
808 in the *qrr*1 promoter regions for every two species. The unweighted pair group method
809 with arithmetic mean (UPGMA) was subsequently used to progressively build a hierarchy
810 of species clusters [78]. In brief, each species was initially represented by one node. At
811 each clustering step, the pair of nodes with the minimal difference score were clustered

into a new node. The arithmetic means of the difference scores between this node pair and each of the other nodes were then assigned to be the difference scores between the newly clustered node and other nodes. The sequence logos were generated by WebLogo [79,80].

Statistical Methods

All statistical analyses were performed using GraphPad Prism software. Error bars correspond to standard deviations of the means of three biological replicates.

Acknowledgements

We thank members of the Bassler laboratory and Dr. Ned Wingreen for insightful discussions and suggestions. This work was supported by the Howard Hughes Medical Institute, National Institutes of Health (NIH) Grant 5R37GM065859, and National Science Foundation Grant MCB-1713731 (to BLB). MJE was supported by NIH graduate training grant NIGMS T32GM007388.

Author Contributions

Conceptualization: MJE BLB.

Data Curation: MJE BLB.

Formal Analysis: MJE CF BLB.

Funding Acquisition: BLB.

Investigation: MJE CF XH.

Project Administration: BLB.

Resources: MJE CF XH BLB.

Supervision: BLB.

Validation: MJE BLB.

Visualization: MJE CF BLB.

Writing – Original Draft Preparation: MJE CF XH BLB.

Writing – Review & Editing: MJE BLB.

Figure Legends

Fig 1. Model of the *V. harveyi* QS system.

(A) LCD and **(B)** HCD. See text for details.

Fig 2. LuxT binds upstream of *luxO,* but it does not repress *luxO.*

(A) EMSAs showing binding of LuxT-6xHis to 95 bp DNA fragments consisting of the *luxO* promoter (left) or control (*E. coli lacZ*) DNA (right). Reaction mixtures contained 20 nM DNA probe and the indicated relative concentrations of the LuxT-6xHis dimer: - = no protein, 1x = 20 nM, 16x = 320 nM. **(B)** Density-dependent bioluminescence emission from WT (black) or Δ*luxT* (blue) *V. harveyi.* Relative light units (RLU) are counts/min mL^{-1} per OD_{600}. Error bars represent standard deviations of the means of $n = 3$ biological replicates. Standard deviations that are smaller than the symbols are not shown. **(C)** qRT-

PCR of *luxO* and *luxC* at LCD (OD_{600} = 0.05) of WT (black) and Δ*luxT* (blue) *V. harveyi*. Error bars represent standard deviations of the means of *n* = 3 biological replicates. Unpaired two-tailed *t* tests with Welch's correction were performed comparing WT to Δ*luxT. p*-values: ns ≥ 0.05, ** < 0.01. **(D)** As in C at HCD (OD_{600} = 1). **(E)** Western blots of AphA-3xFLAG (top) and 3xFLAG-LuxR (3rd panel from top) in WT and Δ*luxT V. harveyi* at LCD (OD_{600} = 0.01) and HCD (OD_{600} = 1). Total proteins were visualized on a stain-free gel before transfer (2nd and bottom panels), and a dominant band serves as a loading control.

Fig 3. LuxT represses *qrr*1 transcription.

(A) Diagram of the *luxO-qrr*1 locus. *qrr*1 resides 151 bp upstream of *luxO* and is transcribed in the opposite direction. The striped green and gray boxes depict the putative LuxO-P and σ^{54} binding sites, respectively. The striped blue box designates the previously identified LuxT binding region, which spans from -76 to -27 relative to the *qrr*1 +1 transcriptional start site. **(B)** Relative fluorescence values (mRuby/OD_{600}) of the indicated *V. harveyi* strains carrying a P_{qrr1}-*mRuby3* transcriptional reporter on a plasmid. Values represent relative fluorescence at OD_{600} = 0.6. **(C)** As in B for strains harboring a P_{luxO}-*mRuby3* reporter. For B and C, unpaired two-tailed *t* tests with Welch's correction were performed comparing mutants to WT. *p* values: ns ≥ 0.05, ** < 0.01, **** < 0.0001. **(D)** qRT-PCR measuring the indicated Qrr sRNAs at OD_{600} = 1. Transcripts were measured in WT (black), Δ*luxT* (blue), *luxO* D61E (green), and *luxO* D61E Δ*luxT* (orange) *V. harveyi*. Different letters indicate significant differences between strains, *p* < 0.05 (two-

878 way analysis of variation (ANOVA) followed by Tukey's multiple comparisons test). For
879 B, C, and D, error bars represent standard deviations of the means of $n = 3$ biological
880 replicates.
881
882 **Fig 4. LuxT activates target genes by two regulatory mechanisms.**
883 **(A)** qRT-PCR of the indicated *VIBHAR_RS* genes in the designated *V. harveyi* strains.
884 The pControl plasmid is the empty parent vector and the plasmid designated p*luxT* carries
885 *luxT* under the IPTG-inducible *tac* promoter. In all cases, 0.5 mM IPTG was added and
886 samples were collected at $OD_{600} = 1$. Error bars represent standard deviations of the
887 means of $n = 3$ biological replicates. Different letters indicate significant differences
888 between strains, $p < 0.05$ (two-way analysis of variation (ANOVA) followed by Tukey's
889 multiple comparisons test). **(B)** Working model for how LuxT activates a target gene, with
890 *VIBHAR_RS11620* as the example in WT *V. harveyi*. **(C)** As in B for Δ*luxT V. harveyi*.
891
892 **Fig 5. LuxT post-transcriptionally activates target genes via repression of *qrr*1.**
893 **(A-D)** Relative fluorescence values (mVenus/OD_{600}) of the indicated *V. harveyi* strains
894 harboring plasmids carrying translational mVenus reporters to the indicated genes. In all
895 cases, 100 ng mL^{-1} aTc was added to induce constitutive transcription of the reporters
896 from the *tetA* promoter. Values represent relative fluorescence at $OD_{600} = 0.3$ for each
897 sample. Error bars represent standard deviations of the means of $n = 3$ biological
898 replicates. Unpaired two-tailed *t* tests with Welch's correction were performed comparing
899 two samples, as indicated. *p*-values: ns ≥ 0.05, ** < 0.01, *** < 0.001. **(E)** Halo formation

by the indicated *V. harveyi* strains on TSA plates containing 5% sheep's blood. Plates were incubated at 30°C for 72 h. A zone of clearing surrounding the colony indicates aerolysin-driven hemolysis.

Fig 6. LuxT represses *qrr*1 in *A. fischeri.*

(A) Simplified *A. fischeri* QS pathway at LCD. See text for details. **(B)** Relative fluorescence values (mRuby3/OD_{600}) of the indicated *A. fischeri* strains carrying a P_{qrr1}-*mRuby3* transcriptional reporter on a plasmid. Values represent relative fluorescence at OD_{600} = 0.6 for each sample. **(C)** *litR* mRNA levels in the designated *A. fischeri* strains at OD_{600} = 1 obtained by qRT-PCR. **(D)** Bioluminescence production of the indicated *A. fischeri* strains at OD_{600} = 1. Relative light units (RLU) are counts/min mL^{-1} per OD_{600}. For B, C, and D, error bars represent standard deviations of the means of n = 3 biological replicates, and unpaired two-tailed t tests with Welch's correction were conducted comparing the WT to the mutants (B) or the two indicated samples (C and D). p-values: ns ≥ 0.05, ** < 0.01, *** < 0.001, **** < 0.0001.

Fig 7. Co-occurrence of *luxT* and *qrr* genes and possible LuxT regulation of *qrr*1 across the *Vibrionaceae*.

(A) Histogram of the number of *qrr* genes in *Vibrio* (purple) and non-*Vibrio* (red) members of the *Vibrionaceae* family. **(B)** Highest similarity score to *V. harveyi luxT* for genes in the indicated genera. The vibrios are divided into three groups based on the number of *qrr* genes in their genomes (indicated by the numbers in the parentheses). The similarity

scores, which quantify the weighted DNA sequence similarities based on the standard scoring matrix NUC44, were obtained from alignments of genome sequences to the query probe using the Smith-Waterman algorithm (see Methods). The black dashed line indicates the cutoff used for the similarity score. Boxes show the means ± SD. Circles represent outlier species whose highest similarity scores to *V. harveyi luxT* fell below the cutoff. **(C)** Alignment of *qrr*1 upstream DNA sequences for the indicated species. Gray and black denote 75% and 100% consensus, respectively. The σ^{54} binding site and the LuxT binding region are indicated. Colors as in Fig 3A. **(D)** Phylogenetic tree of *Vibrionaceae* family members based on the 30 nucleotides upstream of the σ^{54} binding sites in the *qrr*1 promoters. Colors as in panels A and B. Branches corresponding to species shown in panel C are indicated by the circled numbers. Groups of species with highly similar upstream sequences (sequence logos shown on the right) are indicated by letters in parentheses. Regarding the sequence logos, the heights of the different nucleotides are scaled according to their frequencies at each position, and the height of each nucleotide stack is proportional to the information content (measured in bits) of the corresponding position. Scale bar, 1 bit.

References

1. Papenfort K, Bassler BL. Quorum sensing signal-response systems in Gram-negative bacteria. Nat Rev Microbiol. 2016 Aug 11;14(9):576–88.

2. Waters CM, Bassler BL. Quorum sensing: cell-to-cell communication in bacteria. Annu Rev Cell Dev Biol. 2005 Nov;21(1):319–46.

3. Bassler BL, Wright M, Showalter RE, Silverman MR. Intercellular signalling in *Vibrio harveyi*: sequence and function of genes regulating expression of luminescence. Mol Microbiol. 1993 Aug;9(4):773–86.

4. Bassler BL, Wright M, Silverman MR. Multiple signalling systems controlling expression of luminescence in *Vibrio harveyi*: sequence and function of genes encoding a second sensory pathway. Mol Microbiol. 1994 Jul;13(2):273–86.

5. Henke JM, Bassler BL. Quorum sensing regulates type III secretion in *Vibrio harveyi* and *Vibrio parahaemolyticus.* J Bacteriol. 2004 Jun;186(12):3794–805.

6. Lilley BN, Bassler BL. Regulation of quorum sensing in *Vibrio harveyi* by LuxO and Sigma-54. Mol Microbiol. 2000 May;36(4):940–54.

7. Mok KC, Wingreen NS, Bassler BL. *Vibrio harveyi* quorum sensing: a coincidence detector for two autoinducers controls gene expression. EMBO J. 2003 Feb 17;22(4):870–81.

8. van Kessel JC, Rutherford ST, Shao Y, Utria AF, Bassler BL. Individual and combined roles of the master regulators AphA and LuxR in control of the *Vibrio harveyi* quorum-sensing regulon. J Bacteriol. 2013 Feb;195(3):436–43.

961 9. Cao JG, Meighen EA. Purification and structural identification of an autoinducer for
962 the luminescence system of *Vibrio harveyi*. J Biol Chem. 1989 Dec
963 25;264(36):21670–6.

964 10. Surette MG, Miller MB, Bassler BL. Quorum sensing in *Escherichia coli, Salmonella*
965 *typhimurium*, and *Vibrio harveyi*: a new family of genes responsible for autoinducer
966 production. Proc Natl Acad Sci USA. 1999 Feb 16;96(4):1639–44.

967 11. Schauder S, Shokat K, Surette MG, Bassler BL. The LuxS family of bacterial
968 autoinducers: biosynthesis of a novel quorum-sensing signal molecule. Mol
969 Microbiol. 2001 Jul;41(2):463–76.

970 12. Chen X, Schauder S, Potier N, Van Dorsselaer A, Pelczer I, Bassler BL, et al.
971 Structural identification of a bacterial quorum-sensing signal containing boron.
972 Nature. 2002 Jan 31;415(6871):545–9.

973 13. Miller MB, Skorupski K, Lenz DH, Taylor RK, Bassler BL. Parallel quorum sensing
974 systems converge to regulate virulence in *Vibrio cholerae*. Cell. 2002 Aug
975 9;110(3):303–14.

976 14. Henke JM, Bassler BL. Three parallel quorum-sensing systems regulate gene
977 expression in *Vibrio harveyi*. J Bacteriol. 2004 Oct;186(20):6902–14.

978 15. Higgins DA, Pomianek ME, Kraml CM, Taylor RK, Semmelhack MF, Bassler BL.
979 The major *Vibrio cholerae* autoinducer and its role in virulence factor production.
980 Nature. 2007 Dec 6;450(7171):883–6.

16. Ng WL, Perez LJ, Wei Y, Kraml C, Semmelhack MF, Bassler BL. Signal production and detection specificity in *Vibrio* CqsA/CqsS quorum-sensing systems. Mol Microbiol. 2011 Mar;79(6):1407–17.

17. Bassler BL, Wright M, Showalter RE, Silverman MR. Intercellular signalling in *Vibrio harveyi*: sequence and function of genes regulating expression of luminescence. Mol Microbiol. 1993 Aug;9(4):773–86.

18. Freeman JA, Bassler BL. Sequence and function of LuxU: a two-component phosphorelay protein that regulates quorum sensing in *Vibrio harveyi*. J Bacteriol. 1999 Feb;181(3):899–906.

19. Freeman JA, Bassler BL. A genetic analysis of the function of LuxO, a two-component response regulator involved in quorum sensing in *Vibrio harveyi*. Mol Microbiol. 1999 Jan;31(2):665–77.

20. Tu KC, Bassler BL. Multiple small RNAs act additively to integrate sensory information and control quorum sensing in *Vibrio harveyi*. Genes Dev. 2007 Jan 15;21(2):221–33.

21. Lenz DH, Mok KC, Lilley BN, Kulkarni RV, Wingreen NS, Bassler BL. The small RNA chaperone Hfq and multiple small RNAs control quorum sensing in *Vibrio harveyi* and *Vibrio cholerae*. Cell. 2004 Jul 9;118(1):69–82.

22. Showalter RE, Martin MO, Silverman MR. Cloning and nucleotide sequence of *luxR*, a regulatory gene controlling bioluminescence in *Vibrio harveyi*. J Bacteriol. 1990 Jun;172(6):2946–54.

23. Swartzman E, Silverman M, Meighen EA. The *luxR* gene product of *Vibrio harveyi* is a transcriptional activator of the *lux* promoter. J Bacteriol. 1992 Nov;174(22):7490–3.

24. Rutherford ST, van Kessel JC, Shao Y, Bassler BL. AphA and LuxR/HapR reciprocally control quorum sensing in vibrios. Genes Dev. 2011 Feb 15;25(4):397–408.

25. Martin M, Showalter R, Silverman M. Identification of a locus controlling expression of luminescence genes in *Vibrio harveyi*. J Bacteriol. 1989 May;171(5):2406–14.

26. Feng L, Rutherford ST, Papenfort K, Bagert JD, van Kessel JC, Tirrell DA, et al. A Qrr noncoding RNA deploys four different regulatory mechanisms to optimize quorum-sensing dynamics. Cell. 2015 Jan 15;160(1-2):228–40.

27. Shao Y, Bassler BL. Quorum-sensing non-coding small RNAs use unique pairing regions to differentially control mRNA targets. Mol Microbiol. 2012 Feb;83(3):599–611.

28. Freeman JA, Lilley BN, Bassler BL. A genetic analysis of the functions of LuxN: a two-component hybrid sensor kinase that regulates quorum sensing in *Vibrio harveyi*. Mol Microbiol. 2000 Jan;35(1):139–49.

29. Tu KC, Long T, Svenningsen SL, Wingreen NS, Bassler BL. Negative feedback loops involving small regulatory RNAs precisely control the *Vibrio harveyi* quorum-sensing response. Mol Cell. 2010 Feb 26;37(4):567–79.

30. Teng S-W, Schaffer JN, Tu KC, Mehta P, Lu W, Ong NP, et al. Active regulation of receptor ratios controls integration of quorum-sensing signals in *Vibrio harveyi.* Mol Syst Biol. 2011 May 24;7:491.

31. Shao Y, Feng L, Rutherford ST, Papenfort K, Bassler BL. Functional determinants of the quorum-sensing non-coding RNAs and their roles in target regulation. EMBO J. 2013 Jul 31;32(15):2158–71.

32. Lin YH, Miyamoto C, Meighen EA. Purification and characterization of a *luxO* promoter binding protein LuxT from *Vibrio harveyi*. Protein Expr Purif. 2000 Oct;20(1):87–94.

33. Lin YH, Miyamoto C, Meighen EA. Cloning and functional studies of a *luxO* regulator LuxT from *Vibrio harveyi*. Biochim Biophys Acta. 2000 Dec 1;1494(3):226–35.

34. Wang Y, Tu KC, Ong NP, Bassler BL, Wingreen NS. Protein-level fluctuation correlation at the microcolony level and its application to the *Vibrio harveyi* quorum-sensing circuit. Biophys J. 2011 Jun 22;100(12):3045–53.

1037 35. Chaparian RR, Olney SG, Hustmyer CM, Rowe-Magnus DA, van Kessel JC.
1038 Integration host factor and LuxR synergistically bind DNA to coactivate quorum-
1039 sensing genes in *Vibrio harveyi*. Mol Microbiol. 2016 Sep;101(5):823–40.

1040 36. Swartzman E, Meighen EA. Purification and characterization of a poly(dA-dT) *lux*-
1041 specific DNA-binding protein from *Vibrio harveyi* and identification as LuxR. J Biol
1042 Chem. 1993 Aug 5;268(22):16706–16.

1043 37. Miyamoto CM, Smith EE, Swartzman E, Cao JG, Graham AF, Meighen EA.
1044 Proximal and distal sites bind LuxR independently and activate expression of the
1045 *Vibrio harveyi lux* operon. Mol Microbiol. 1994 Oct;14(2):255–62.

1046 38. van Kessel JC, Ulrich LE, Zhulin IB, Bassler BL. Analysis of activator and repressor
1047 functions reveals the requirements for transcriptional control by LuxR, the master
1048 regulator of quorum sensing in *Vibrio harveyi*. mBio. 2013 Jul 9;4(4):e00378–13.

1049 39. Jaques S, McCarter LL. Three new regulators of swarming in *Vibrio*
1050 *parahaemolyticus*. J Bacteriol. 2006 Apr;188(7):2625–35.

1051 40. Howard SP, Buckley JT. Membrane glycoprotein receptor and hole-forming
1052 properties of a cytolytic protein toxin. Biochemistry. 1982 Mar 30;21(7):1662–7.

1053 41. Boyaci H, Shah T, Hurley A, Kokona B, Li Z, Ventocilla C, et al. Structure, regulation,
1054 and inhibition of the quorum-sensing signal integrator LuxO. PLoS Biol. 2016 May
1055 24;14(5):e1002464.

1056 42. Roh J-B, Lee M-A, Lee H-J, Kim S-M, Cho Y, Kim Y-J, et al. Transcriptional
1057 regulatory cascade for elastase production in *Vibrio vulnificus*: LuxO activates *luxT*
1058 expression and LuxT represses *smcR* expression. J Biol Chem. 2006 Nov
1059 17;281(46):34775–84.

1060 43. Liu H, Gu D, Cao X, Liu Q, Wang Q, Zhang Y. Characterization of a new quorum
1061 sensing regulator LuxT and its roles in the extracellular protease production, motility,
1062 and virulence in fish pathogen *Vibrio alginolyticus*. Arch Microbiol. 2012
1063 Jun;194(6):439–52.

1064 44. Eickhoff MJ, Bassler BL. *Vibrio fischeri* siderophore production drives competitive
1065 exclusion during dual-species growth. Mol Microbiol. 2020 Aug;114(2):244–61.

1066 45. Miyashiro T, Wollenberg MS, Cao X, Oehlert D, Ruby EG. A single *qrr* gene is
1067 necessary and sufficient for LuxO-mediated regulation in *Vibrio fischeri*. Mol
1068 Microbiol. 2010 Sep;77(6):1556–67.

1069 46. Fidopiastis PM, Miyamoto CM, Jobling MG, Meighen EA, Ruby EG. LitR, a new
1070 transcriptional activator in *Vibrio fischeri,* regulates luminescence and symbiotic
1071 light organ colonization. Mol Microbiol. 2002 Jul;45(1):131–43.

1072 47. Stocker R, Seymour JR. Ecology and physics of bacterial chemotaxis in the ocean.
1073 Microbiol Mol Biol Rev. 2012 Dec;76(4):792–812.

48. Sunagawa S, Coelho LP, Chaffron S, Kultima JR, Labadie K, Salazar G, et al. Ocean plankton. Structure and function of the global ocean microbiome. Science. 2015 May 22;348(6237):1261359.

49. Gottesman S. Trouble is coming: Signaling pathways that regulate general stress responses in bacteria. J Biol Chem. 2019 Aug 2;294(31):11685–700.

50. Bruger EL, Waters CM. Bacterial quorum sensing stabilizes cooperation by optimizing growth strategies. Appl Environ Microbiol. 2016 Oct 27;82(22):6498–506.

51. Svenningsen SL. Small RNA-based regulation of bacterial quorum sensing and biofilm formation. Microbiol Spectr. 2018 Jul;6(4).

52. Storz G, Vogel J, Wassarman KM. Regulation by small RNAs in bacteria: expanding frontiers. Mol Cell. 2011 Sep 16;43(6):880–91.

53. Gottesman S, Storz G. Bacterial small RNA regulators: versatile roles and rapidly evolving variations. Cold Spring Harb Perspect Biol. 2011 Dec 1;3(12):a003798.

54. Beisel CL, Storz G. The base-pairing RNA Spot 42 participates in a multioutput feedforward loop to help enact catabolite repression in *Escherichia coli*. Mol Cell. 2011 Feb 4;41(3):286–97.

55. Shao Y, Bassler BL. Quorum regulatory small RNAs repress type VI secretion in *Vibrio cholerae*. Mol Microbiol. 2014 Jun;92(5):921–30.

1092 56. Ng WL, Perez L, Cong J, Semmelhack MF, Bassler BL. Broad spectrum pro-
1093 quorum-sensing molecules as inhibitors of virulence in vibrios. PLoS Pathog.
1094 2012;8(6):e1002767.

1095 57. Milton DL. Quorum sensing in vibrios: complexity for diversification. Int J Med
1096 Microbiol. 2006 Apr;296(2-3):61–71.

1097 58. Ng WL, Bassler BL. Bacterial quorum-sensing network architectures. Annu Rev
1098 Genet. 2009;43:197–222.

1099 59. Ramos JL, Martínez-Bueno M, Molina-Henares AJ, Terán W, Watanabe K, Zhang
1100 X, et al. The TetR family of transcriptional repressors. Microbiol Mol Biol Rev. 2005
1101 Jun;69(2):326–56.

1102 60. Allen RD, Baumann P. Structure and arrangement of flagella in species of the
1103 genus *Beneckea* and *Photobacterium fischeri*. J Bacteriol. 1971 Jul;107(1):295–
1104 302.

1105 61. Shinoda S, Okamoto K. Formation and function of *Vibrio parahaemolyticus* lateral
1106 flagella. J Bacteriol. 1977 Mar;129(3):1266–71.

1107 62. McCarter L, Hilmen M, Silverman M. Flagellar dynamometer controls swarmer cell
1108 differentiation of *V. parahaemolyticus*. Cell. 1988 Jul 29;54(3):345–51.

1109 63. Bassler BL, Greenberg EP, Stevens AM. Cross-species induction of luminescence
1110 in the quorum-sensing bacterium *Vibrio harveyi*. J Bacteriol. 1997
1111 Jun;179(12):4043–5.

64. Boettcher KJ, Ruby EG. Depressed light emission by symbiotic *Vibrio fischeri* of the sepiolid squid *Euprymna scolopes*. J Bacteriol. 1990 Jul;172(7):3701–6.

65. Thelin KH, Taylor RK. Toxin-coregulated pilus, but not mannose-sensitive hemagglutinin, is required for colonization by *Vibrio cholerae* O1 El Tor biotype and O139 strains. Infect Immun. 1996 Jul;64(7):2853–6.

66. McCarter LL. OpaR, a homolog of *Vibrio harveyi* LuxR, controls opacity of *Vibrio parahaemolyticus*. J Bacteriol. 1998 Jun;180(12):3166–73.

67. Greenberg EP, Hastings JW, Ulitzur S. Induction of luciferase synthesis in *Beneckea harveyi* by other marine bacteria. Arch Microbiol. 1979 Feb;120(2):87–91.

68. Gibson DG, Young L, Chuang RY, Venter JC, Hutchison CA, Smith HO. Enzymatic assembly of DNA molecules up to several hundred kilobases. Nat Methods. 2009 May;6(5):343–5.

69. Bina XR, Wong EA, Bina TF, Bina JE. Construction of a tetracycline inducible expression vector and characterization of its use in *Vibrio cholerae.* Plasmid. 2014 Nov;76:87–94.

70. Edwards RA, Keller LH, Schifferli DM. Improved allelic exchange vectors and their use to analyze 987P fimbria gene expression. Gene. 1998 Jan 30;207(2):149–57.

71. Papenfort K, Silpe JE, Schramma KR, Cong J-P, Seyedsayamdost MR, Bassler BL. A *Vibrio cholerae* autoinducer-receptor pair that controls biofilm formation. Nat Chem Biol. 2017 May;13(5):551–7.

72. Bernheimer AW. Assay of hemolytic toxins. Methods Enzymol. 1988;165:213–7.

73. Bezar IF, Mashruwala AA, Boyd JM, Stock AM. Drug-like fragments inhibit agr-mediated virulence expression in *Staphylococcus aureus*. Sci Rep. 2019 May 1;9(1):6786.

74. Benson DA, Karsch-Mizrachi I, Lipman DJ, Ostell J, Rapp BA, Wheeler DL. GenBank. Nucleic Acids Res. 2000 Jan 1;28(1):15–8.

75. Smith TF, Waterman MS. Identification of common molecular subsequences. J Mol Biol. 1981 Mar 25;147(1):195–7.

76. Notredame C, Higgins DG, Heringa J. T-Coffee: A novel method for fast and accurate multiple sequence alignment. J Mol Biol. 2000 Sep 8;302(1):205–17.

77. Jukes TH, Cantor CR. Evolution of protein molecules. In: Munro HN, editor. Mammalian protein metabolism. New York: Academic Press; 1969. pp. 21–132.

78. Sokal RR, Michener C. A statistical method for evaluating systematic relationships. Univ Kansas, Sci Bull. 1958;38:1409–38.

79. Schneider TD, Stephens RM. Sequence logos: a new way to display consensus sequences. Nucleic Acids Res. 1990 Oct 25;18(20):6097–100.

80. Crooks GE, Hon G, Chandonia J-M, Brenner SE. WebLogo: a sequence logo generator. Genome Res. 2004 Jun;14(6):1188–90.

Supporting Information Captions

S1 Table. Strains used in this study.

S2 Table. Oligonucleotides used in this study.

S3 Table. Plasmids used in this study.

S1 Fig. LuxT binds upstream of *luxO*.

EMSA showing binding of LuxT-6xHis to 95 bp DNA fragments containing the WT *luxO* promoter (left) and the *luxO* promoter in which the 50 nucleotides previously shown to be crucial for LuxT binding were randomized (right). DNA and protein concentrations as in Fig 2A.

S2 Fig. The *luxO-qrr*1 locus.

The *V. harveyi* genomic DNA region harboring the LuxO-P, LuxT, and σ^{54} binding sites. The sites are labeled in relation to the *qrr*1 +1 transcriptional start site, which is also designated. Colors as in Fig 3A.

S3 Fig. LuxT does not repress *qrr*2-5.

(A) Relative fluorescence values (mRuby3/OD_{600}) of the indicated *V. harveyi* strains harboring a plasmid-borne P_{qrr2}-*mRuby3* transcriptional reporter. Values represent

1169 relative fluorescence at OD_{600} = 0.6 for each sample. **(B-D)** As in A, except the strains
1170 harbor P_{qrr3}-*mRuby3,* P_{qrr4}-*mRuby3,* and P_{qrr5}-*mRuby3*, respectively. In all panels, error
1171 bars represent standard deviations of the means of *n* = 3 biological replicates. Unpaired
1172 two-tailed *t* tests with Welch's correction were performed comparing the indicated two
1173 samples. *p*-values: ns ≥ 0.05.
1174
1175 **S4 Fig. LuxT activates *luxCDABE* independently of Qrr1.**
1176 Density-dependent bioluminescence production from WT (black), Δ*luxT* (blue), Δ*qrr*1
1177 (green), and Δ*qrr*1 Δ*luxT* (orange) *V. harveyi* strains. Relative light units (RLU) are
1178 counts/min mL^{-1} per OD_{600}. Error bars represent standard deviations of the means of *n* =
1179 3 biological replicates.
1180
1181 **S5 Fig. LuxT does not bind the *luxCDABE* promoter.**
1182 **(A)** Diagram of the *luxCDABE* promoter region. Black striped boxes represent known
1183 LuxR binding sites. The black lines labeled 1 to 6 show the ~100 bp overlapping DNA
1184 fragments that were amplified and used as probes. The probes span the region -405 to
1185 +81 relative to the *luxC* start codon. (Figure adapted from Chaparian, *et al.* 2016 [35]).
1186 **(B-D)** EMSAs measuring LuxT-6xHis binding to Probes 1-6 from panel A. DNA and
1187 protein concentrations as in Fig 2A.
1188
1189 **S6 Fig. LuxT does not directly activate *luxCDABE* in *E. coli.***

(A) Bioluminescence production from *E. coli* BW25113 harboring *luxCDABE* expressed from its native promoter on a plasmid (pBB1). The *E. coli* carries two additional plasmids, as indicated. - denotes the empty parent vector. + denotes the p*luxR* and/or the p*luxT* plasmid, encoding IPTG inducible *luxR* and arabinose inducible *luxT,* respectively. Strains were grown for 16 h in LB containing 0.5 mM IPTG in the absence (black) or presence (gray) of 0.2% arabinose. Relative light units (RLU) are counts/min mL^{-1} per OD_{600}. **(B)** qRT-PCR measurements of *luxT* transcript levels in the *E. coli* strains harboring the p*luxT* plasmid from panel A. **(C)** Cell densities (OD_{600}) of the strains in panel A after 24 h of growth. For panels B and C, the labeling and color schemes are as in panel A. In all panels, error bars represent standard deviations of the means of n = 3 biological replicates.

S7 Fig. LuxT activation of *luxCDABE* does not depend on known QS genes.

(A-D) Density-dependent bioluminescence production from the designated *V. harveyi* strains that possess (black) and lack (blue) *luxT.* Relative light units (RLU) are counts/min mL^{-1} per OD_{600}. Error bars represent standard deviations of the means of n = 3 biological replicates.

S8 Fig. LuxT does not regulate *luxR* and *aphA*.

qRT-PCR measurements of *luxR* and *aphA* transcript levels in WT (black) and Δ*luxT* (blue) *V. harveyi* at LCD (OD_{600} = 0.05). Error bars represent standard deviations of the

means of $n = 3$ biological replicates. Unpaired two-tailed *t* tests with Welch's correction were performed comparing WT to Δ*luxT*. *p*-values: ns ≥ 0.05.

S9 Fig. LuxT activates Qrr target mRNAs independently of Qrr1.

(A) Transcript levels of the indicated *VIBHAR_RS* genes as measured by qRT-PCR in *V. harveyi luxO* D61E and *V. harveyi luxO* D61E Δ*luxT* strains at $OD_{600} = 1$. Unpaired two-tailed *t* tests with Welch's correction were performed comparing *V. harveyi luxO* D61E to *V. harveyi luxO* D61E Δ*luxT*. *p*-values: ns ≥ 0.05, ** < 0.01, *** < 0.001, **** < 0.0001. **(B)** qRT-PCR measurements of transcript levels of the indicated *VIBHAR_RS* genes in the designated *V. harveyi* strains at $OD_{600} = 1$. Different letters indicate significant differences between strains, $p < 0.05$ (two-way analysis of variation (ANOVA) followed by Tukey's multiple comparisons test). In both panels, error bars represent standard deviations of the means of $n = 3$ biological replicates.

S10 Fig. LuxT activates the transcription of the target genes.

Activities of *lux* transcriptional fusions to the indicated promoters were measured in the designated *V. harveyi* strains at $OD_{600} = 1$. Relative light units (RLU) are counts/min mL^{-1} per OD_{600}. Error bars represent standard deviations of $n = 3$ biological replicates. Unpaired two-tailed *t* tests with Welch's correction were performed comparing *V. harveyi luxA*::Tn*5* to *V. harveyi luxA*::Tn*5* Δ*luxT*. *p*-values: ** < 0.01, **** < 0.0001.

S11 Fig. Qrr1 overexpression represses translational reporter constructs.

Relative fluorescence (mVenus/OD_{600}) of WT *V. harveyi* harboring a plasmid encoding a translational reporter to the indicated *VIBHAR_RS* gene transcribed from the aTc inducible *tetA* promoter. The *V. harveyi* strains also carry IPTG-inducible *qrr*1 on a plasmid (p*qrr*1) or the empty parent vector (pControl). All strains were grown in the presence of 0.5 mM IPTG. Strains were grown in the absence and presence of 100 ng mL^{-1} aTc (- aTc and + aTc, respectively). Values represent relative fluorescence at OD_{600} = 0.3 for each sample. Error bars represent standard deviations of the means of $n = 3$ biological replicates. Different letters indicate significant differences between strains, $p < 0.05$ (two-way analysis of variation (ANOVA) followed by Tukey's multiple comparisons test).

S12 Fig. LuxT and Qrr1 control aerolysin production.

Hemolytic activity present in the indicated *V. harveyi* cell-free culture fluids as judged by lysis of defibrinated sheep's blood. Culture fluids were collected after 24 h of growth in AB medium. Hemolytic activity was normalized to the activity of ddH_2O [A_{415}(sample)/A_{415}(ddH_2O) x 100]. Error bars represent standard deviations of the means of $n = 3$ biological replicates. Unpaired two-tailed *t* tests with Welch's correction were performed comparing two samples, as indicated. *p*-values: *** < 0.001, **** < 0.0001.

S13 Fig. LuxT does not appear to control *qrr*1 in *V. cholerae* or *V. parahaemolyticus.*

(A) Activity of a *V. cholerae* P_{qrr1}-*luxCDABE* transcriptional reporter in the indicated *V. cholerae* strains. **(B)** Relative fluorescence of a *V. parahaemolyticus* P_{qrr1}-*mRuby3*

transcriptional reporter measured in the indicated *V. parahaemolyticus* strains. Relative light production (panel A) and relative fluorescence (panel B) represent values when OD_{600} = 0.6 for each sample. Error bars represent standard deviations of the means of *n* = 3 biological replicates. Unpaired two-tailed *t* tests with Welch's correction were performed comparing two samples, as indicated. *p*-values: ns ≥ 0.05.

S1 Data. Numerical data for Figs 2B, 2C, 2D, 3B, 3C, 3D, 4A, 5A, 5B, 5C, 5D, 6B, 6C, 6D, 7A, and 7B.

S2 Data. Numerical data for S3A, S3B, S3C, S3D, S4, S6A, S6B, S6C, S7A, S7B, S7C, S7D, S8, S9A, S9B, S10, S11, S12, S13A, and S13B Figs.

Fig 1

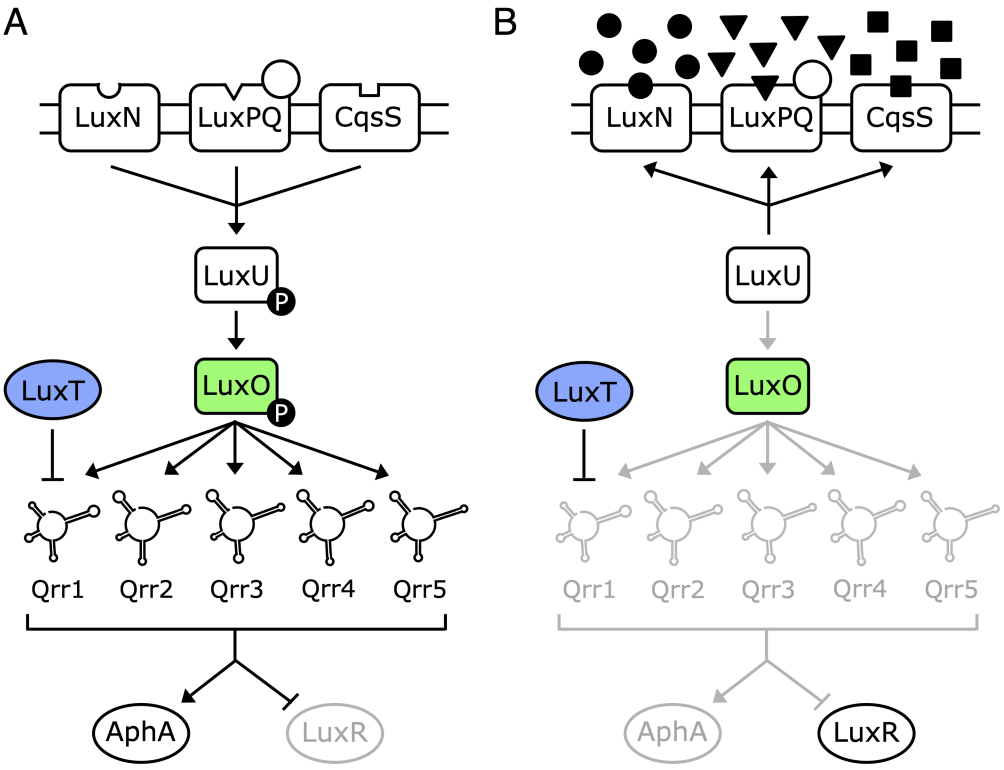
A
LuxN
LuxPQ
CqsS
LuxU
P
LuxO
P
LuxT
Qrr1
Qrr2
Qrr3
Qrr4
Qrr5
AphA
LuxR
B
LuxN
LuxPQ
CqsS
LuxU
LuxO
LuxT
Qrr1
Qrr2
Qrr3
Qrr4
Qrr5
AphA
LuxR

Fig 2

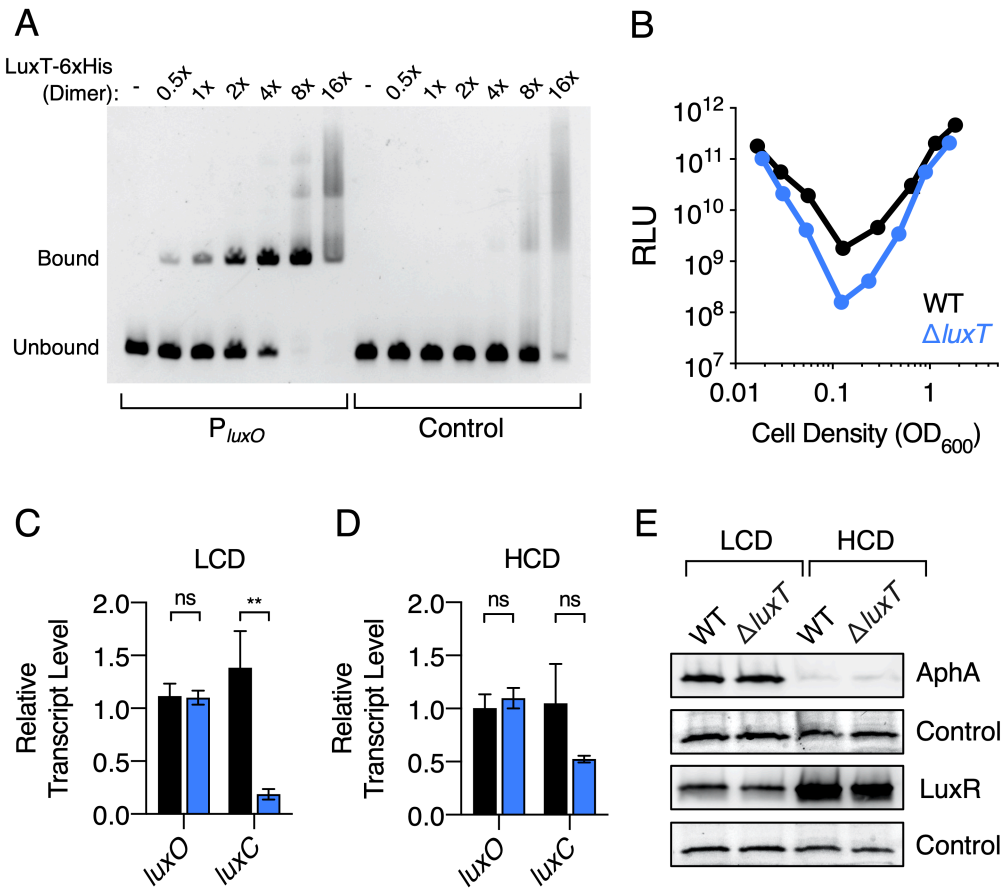
A
LuxT-6xHis
(Dimer): - 0.5x 1x 2x 4x 8x 16x - 0.5x 1x 2x 4x 8x 16x
Bound
Unbound
P luxO
Control
B
RLU
10^12
10^11
10^10
10^9
10^8
10^7
0.01
0.1
1
Cell Density (OD600)
WT
ΔluxT
C
LCD
Relative Transcript Level
2.0
1.5
1.0
0.5
0.0
ns
**
luxO
luxC
D
HCD
Relative Transcript Level
ns
ns
luxO
luxC
E
LCD
HCD
WT
ΔluxT
WT
ΔluxT
AphA
Control
LuxR
Control

Fig 3

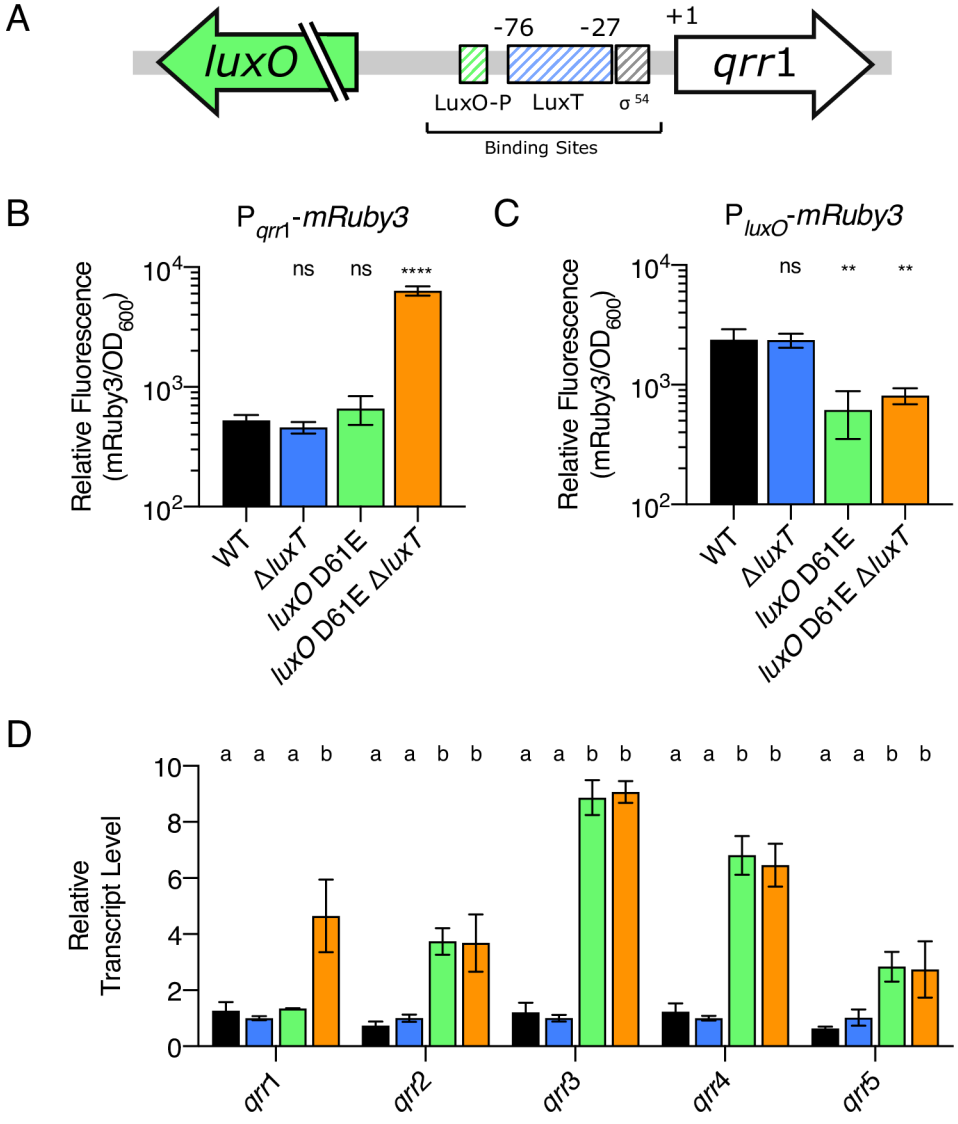
A
luxO
-76
-27
+1
qrr1
LuxO-P
LuxT
σ 54
Binding Sites
B
P qrr1-mRuby3
Relative Fluorescence (mRuby3/OD600)
ns
ns
****
WT
ΔluxT
luxO D61E
luxO D61E ΔluxT
C
P luxO-mRuby3
ns
**
**
D
Relative Transcript Level
a a a b a a b b a a b b a a b b a a b b
qrr1
qrr2
qrr3
qrr4
qrr5

Fig 4

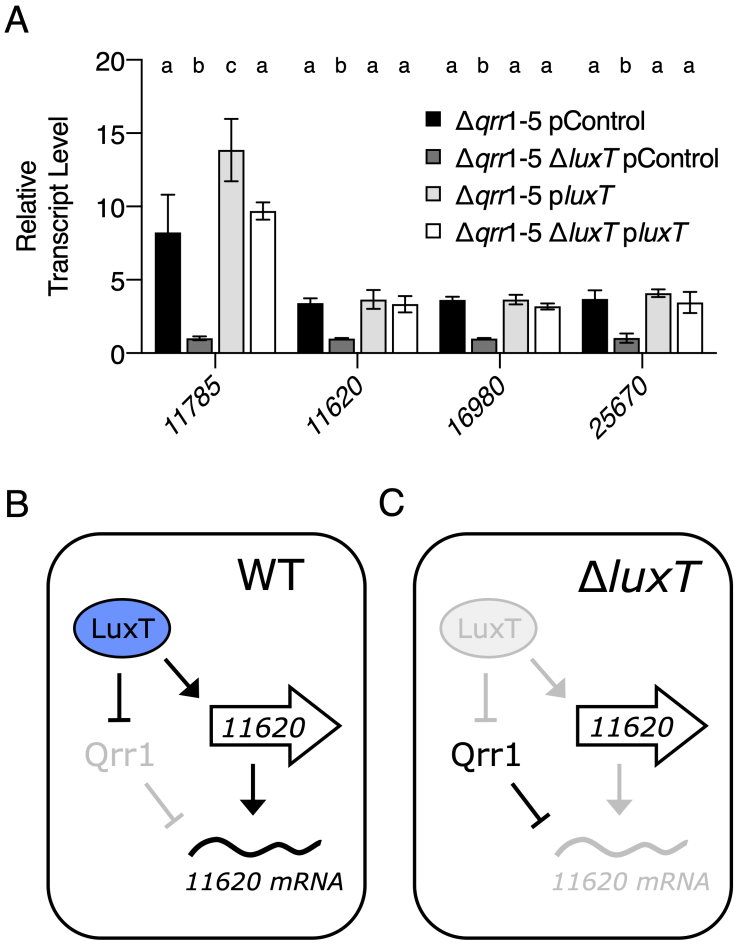
A
a b c a a b a a a b a a a b a a
20
15
10
5
0
Relative Transcript Level
Δqrr1-5 pControl
Δqrr1-5 ΔluxT pControl
Δqrr1-5 pluxT
Δqrr1-5 ΔluxT pluxT
11785
11620
16980
25670
B
WT
LuxT
Qrr1
11620
11620 mRNA
C
ΔluxT
LuxT
Qrr1
11620
11620 mRNA

Fig 5

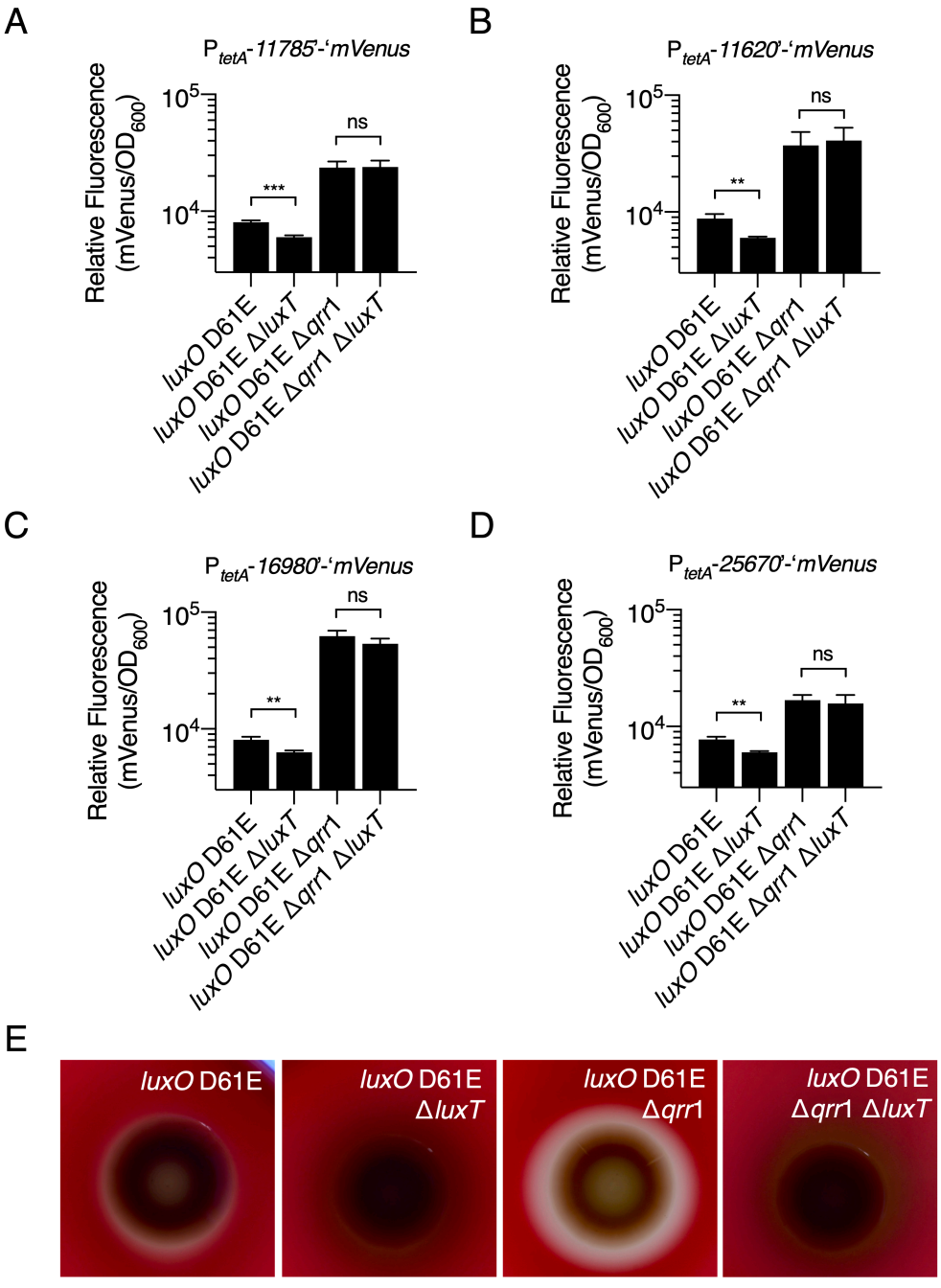
A
P tetA-11785'-'mVenus
Relative Fluorescence (mVenus/OD600)
10^5
10^4
***
ns
luxO D61E
luxO D61E ΔluxT
luxO D61E Δqrr1
luxO D61E Δqrr1 ΔluxT
B
P tetA-11620'-'mVenus
Relative Fluorescence (mVenus/OD600)
10^5
10^4
**
ns
luxO D61E
luxO D61E ΔluxT
luxO D61E Δqrr1
luxO D61E Δqrr1 ΔluxT
C
P tetA-16980'-'mVenus
Relative Fluorescence (mVenus/OD600)
10^5
10^4
**
ns
luxO D61E
luxO D61E ΔluxT
luxO D61E Δqrr1
luxO D61E Δqrr1 ΔluxT
D
P tetA-25670'-'mVenus
Relative Fluorescence (mVenus/OD600)
10^5
10^4
**
ns
luxO D61E
luxO D61E ΔluxT
luxO D61E Δqrr1
luxO D61E Δqrr1 ΔluxT
E
luxO D61E
luxO D61E ΔluxT
luxO D61E Δqrr1
luxO D61E Δqrr1 ΔluxT

Fig 6

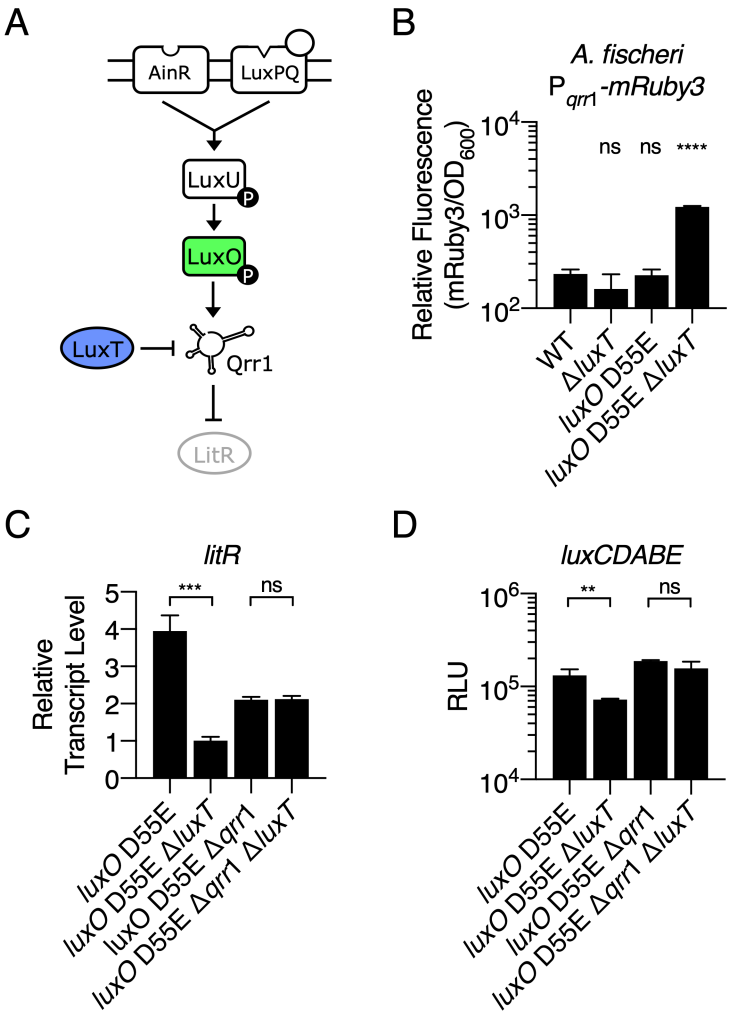
A
AinR
LuxPQ
LuxU
P
LuxO
P
LuxT
Qrr1
LitR
B
A. fischeri
P qrr1 -mRuby3
Relative Fluorescence
(mRuby3/OD600)
10^4
10^3
10^2
ns
ns
****
WT
ΔluxT
luxO D55E
luxO D55E ΔluxT
C
litR
Relative
Transcript Level
5
4
3
2
1
0
***
ns
luxO D55E
luxO D55E ΔluxT
luxO D55E Δqrr1
luxO D55E Δqrr1 ΔluxT
D
luxCDABE
RLU
10^6
10^5
10^4
**
ns
luxO D55E
luxO D55E ΔluxT
luxO D55E Δqrr1
luxO D55E Δqrr1 ΔluxT

Fig 7

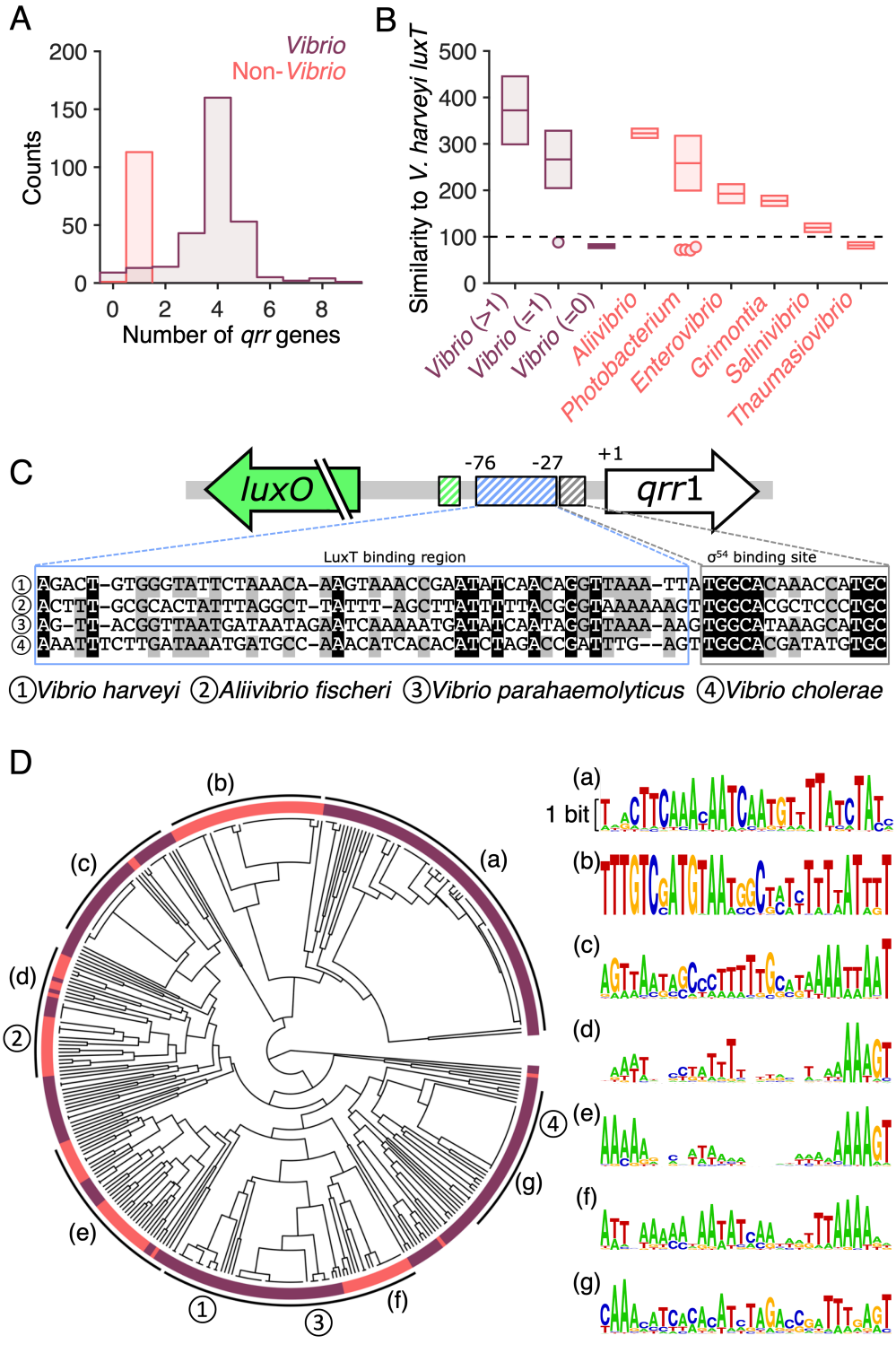
A
Vibrio
Non-Vibrio
Counts
Number of qrr genes
B
Similarity to V. harveyi luxT
Vibrio (>1)
Vibrio (=1)
Vibrio (=0)
Aliivibrio
Photobacterium
Enterovibrio
Grimontia
Salinivibrio
Thaumasiovibrio
C
luxO
qrr1
-76
-27
+1
LuxT binding region
σ54 binding site
①Vibrio harveyi ②Aliivibrio fischeri ③Vibrio parahaemolyticus ④Vibrio cholerae
D
1 bit

S1 Table. Strains used in this study

(WT strains are depicted in bold with variants listed below them.)

Strain	Relevant genotype or feature	Reference
***V. harveyi* BB120**	WT	[1]
ME287	Δ*luxT*	This study
ME790	*aphA-3xFLAG*	This study
ME791	*aphA-3xFLAG* Δ*luxT*	This study
ME792	*3xFLAG-luxR*	This study
ME793	*3xFLAG-luxR* Δ*luxT*	This study
JSV780	*luxO* D61E	[2]
ME181	*luxO* D61E Δ*luxT*	This study
KT39	Δ*qrr*1	[3]
ME431	Δ*qrr*1 Δ*luxT*	This study
KT282	Δ*qrr*1-5	[3]
ME794	Δ*qrr*1-5 Δ*luxT*	This study
BB721	Δ*luxO*	[4]
ME393	Δ*luxO* Δ*luxT*	This study
ME291	Δ*VIBHAR_RS03920*	This study
ME302	Δ*VIBHAR_RS03920* Δ*luxT*	This study
ME795	*luxO* D61E Δ*qrr*1	This study
ME796	*luxO* D61E Δ*qrr*1 Δ*luxT*	This study
BH421	*luxA*::Tn*5*	[5]
ME911	*luxA*::Tn*5* Δ*luxT*	This study
***Vibrio cholerae* C6706**	WT	[6]
ME651	Δ*luxT*	This study
SLS340	*luxO* D61E	[7]
ME797	*luxO* D61E Δ*luxT*	This study
***V. parahaemolyticus* BB22OP**	WT	[8]
ME798	Δ*swrT*	This study
ME799	*luxO* D61E	This study
ME800	*luxO* D61E Δ*swrT*	This study
***A. fischeri* ES114**	WT	[9]
ME226	Δ*luxT*	[10]
ME801	*luxO* D55E	This study
ME802	*luxO* D55E Δ*luxT*	This study
ME803	*luxO* D55E Δ*qrr*1	This study
ME804	*luxO* D55E Δ*qrr*1 Δ*luxT*	This study
E. coli* S17-1 λ*pir	WT	[11]
***E. coli* BL21 (DE3)**	*E. coli str. B, F- ompT hsdSB (rBmB-) gal dcm (DE3)*	Agilent
***E. coli* BW25113**	$lacI^q$ $rrnB_{T14}$ Δ$lacZ_{WJ16}$ *hsdR514* Δ*araBAD*$_{AH33}$ Δ*rhaBAD*$_{LD78}$	[12]

Table S1 References

1. Bassler BL, Greenberg EP, Stevens AM. Cross-species induction of luminescence in the quorum-sensing bacterium *Vibrio harveyi*. J Bacteriol. 1997 Jun;179(12):4043–5.

2. Freeman JA, Bassler BL. A genetic analysis of the function of LuxO, a two-component response regulator involved in quorum sensing in *Vibrio harveyi*. Mol Microbiol. 1999 Jan;31(2):665–77.

3. Tu KC, Bassler BL. Multiple small RNAs act additively to integrate sensory information and control quorum sensing in *Vibrio harveyi*. Genes Dev. 2007 Jan 15;21(2):221–33.

4. Henke JM, Bassler BL. Quorum sensing regulates type III secretion in *Vibrio harveyi* and *Vibrio parahaemolyticus*. J Bacteriol. 2004 Jun;186(12):3794–805.

5. Waters CM, Wu JT, Ramsey ME, Harris RC, Bassler BL. Control of the type 3 secretion system in *Vibrio harveyi* by quorum sensing through repression of ExsA. Appl Environ Microbiol. 2010 Aug;76(15):4996–5004.

6. Thelin KH, Taylor RK. Toxin-coregulated pilus, but not mannose-sensitive hemagglutinin, is required for colonization by *Vibrio cholerae* O1 El Tor biotype and O139 strains. Infect Immun. 1996 Jul;64(7):2853–6.

7. Waters CM, Lu W, Rabinowitz JD, Bassler BL. Quorum sensing controls biofilm formation in *Vibrio cholerae* through modulation of cyclic di-GMP levels and repression of vpsT. J Bacteriol. 2008 Apr;190(7):2527–36.

8. McCarter LL. OpaR, a homolog of *Vibrio harveyi* LuxR, controls opacity of *Vibrio parahaemolyticus*. J Bacteriol. 1998 Jun;180(12):3166–73.

9. Boettcher KJ, Ruby EG. Depressed light emission by symbiotic *Vibrio fischeri* of the sepiolid squid *Euprymna scolopes*. J Bacteriol. 1990 Jul;172(7):3701–6.

10. Eickhoff MJ, Bassler BL. *Vibrio fischeri* siderophore production drives competitive exclusion during dual-species growth. Mol Microbiol. 2020 Aug;114(2):244–61.

11. de Lorenzo V, Timmis KN. Analysis and construction of stable phenotypes in gram-negative bacteria with Tn5- and Tn10-derived minitransposons. Methods Enzymol. 1994;235:386–405.

12. Datsenko KA, Wanner BL. One-step inactivation of chromosomal genes in *Escherichia coli* K-12 using PCR products. Proc Natl Acad Sci USA. 2000 Jun 6;97(12):6640–5.

S2 Table. Oligonucleotides used in this study
Sequences are provided in the 5' → 3' direction

Name	Sequence	Description
ME-633	GGTATATCTCCTTCTTAAAGTTAAACAAAATTATT	Plasmid construction, pET15b cloning
ME-690	GCAGCTGCGCATCATCATCATCATCACTAACAAAGCCCGAAAGGAAGCTG	Plasmid construction, pET15b-*6xHis* cloning
ME-635	TTTTGTTTAACTTTAAGAAGGAGATATACCATGCCAAAGCGTAGTAAAGAAGATAC	Plasmid construction, pET15b-*luxT-6xHis*
ME-691	TTAGTGATGATGATGATGATGCGCAGCTGCTTTGCTCATTTGAATTAACGAACG	Plasmid construction, pET15b-*luxT-6xHis*
ME-924	GTGCCATAATTTAACCTGTTGATATTCG	P_{luxO} EMSA probe forward primer
ME-708	TCGCATTACGCTTTGCATTTTG	P_{luxO} EMSA probe reverse primer
ME-920	ATGGCGCTTTGCCTGGTTTC	$P_{Control}$ EMSA probe forward primer (from *E. coli* MG1655)
ME-927	TTGAGGGGACGACGACAGTATC	$P_{Control}$ EMSA probe reverse primer (from *E. coli* MG1655)
pRE112-F	ATGCAGTTCACTTACACCGCTTC	Plasmid construction, pRE112 mediated chromosomal alterations
pRE112-R	GGGATCGGGCCCTATCACTT	Plasmid construction, pRE112 mediated chromosomal alterations
ME-121	GGGTTGAGAAGCGGTGTAAGTGAACTGCATTGTGCTACTGATGTGTACCGATG	Plasmid construction, *luxT* deletion (*V. harveyi)*
ME-122	TGGCATATTTTAAGCTCTTCTCTTTG	Plasmid construction, *luxT* deletion (*V. harveyi)*
ME-123	TTTACAAAGAGAAGAGCTTAAAATATGCCATAACACTAGAACAAGAAAGCCCCG	Plasmid construction, *luxT* deletion (*V. harveyi)*
ME-124	ACGCCTGAATAAGTGATAGGGCCCGATCCCGTACACTGCTTCCTATCTCAGC	Plasmid construction, *luxT* deletion (*V. harveyi)*
STR-0040	CGTGAGCGTATCCCGGTATCTAT	qRT-PCR, *hfq* (*V. harveyi)*
STR-0041	TTGCAGTTTGATACCGTTCACAAG	qRT-PCR, *hfq* (*V. harveyi)*
ME-255	ACAGCCCATGGTTCTATCGATAC	qRT-PCR, *luxO* (*V. harveyi)*
ME-256	CTTTACGGATCGCATTGTTCACC	qRT-PCR, *luxO* (*V. harveyi)*
ME-416	TATACAACAGGGCAGCGTTGG	qRT-PCR, *luxC* (*V. harveyi)*

ME-417	TCCAATTTGCTTCGAGTTTCGC	qRT-PCR, *luxC* (*V. harveyi)*
ME-871	GGGTTGAGAAGCGGTGTAAGTGAACTGCATTTAGAAGAAGCATTGATGGTGACG	Plasmid construction, pRE112-*aphA-3xFLAG*
ME-872	CCCATCGTGATCTTTGTAGTCTCCCAGTGCGCCGATCACTTCAAGTTCTGTTAG	Plasmid construction, pRE112-*aphA-3xFLAG*
ME-873	GCACTGGGAGACTACAAAGATCACGATGGGGATT	Plasmid construction, pRE112-*aphA-3xFLAG*
ME-560	TTTGTCGTCGTCATCCTTGTAGTC	Plasmid construction, pRE112-*aphA-3xFLAG*
ME-874	ATATCGACTACAAGGATGACGACGACAAATAATTCGTCACTTTAAATAAAACGAAAAAGG	Plasmid construction, pRE112-*aphA-3xFLAG*
ME-875	ACGCCTGAATAAGTGATAGGGCCCGATCCCTTTGAGGAATTTTGATTTCGTGGTGG	Plasmid construction, pRE112-*aphA-3xFLAG*
ME-865	GGGTTGAGAAGCGGTGTAAGTGAACTGCATACTCAAAAGAGACCGTGGAAGC	Plasmid construction, pRE112-*3xFLAG-luxR*
ME-866	CTTGTAATCCCCATCGTGATCCTTGTAGTCCATATTTCTTTTTCCTTGCCATTTGAG	Plasmid construction, pRE112-*3xFLAG-luxR*
ME-867	GACTACAAGGATCACGATGGGGATT	Plasmid construction, pRE112-*3xFLAG-luxR*
ME-564	TCCCAGTGCTTTGTCGTCGTCATCCTTGTAGTC	Plasmid construction, pRE112-*3xFLAG-luxR*
ME-868	TACAAGGATGACGACGACAAAGCACTGGGAGACTCAATTGCAAAGAGACCTCG	Plasmid construction, pRE112-*3xFLAG-luxR*
ME-869	ACGCCTGAATAAGTGATAGGGCCCGATCCCAAGTATTTGAAGGCTCAATCACTGAC	Plasmid construction, pRE112-*3xFLAG-luxR*
ME-601	GTGAAGGGCAATCAGCTGTTG	Plasmid construction, transcriptional reporters in pFED343
ME-444	TCACTACTCTGTGCTATGGTGTTC	Plasmid construction, cloning in pFED343
ME-524	TGAGACGGGCAACAGCTGATTGCCCTTCACAAAAGTATACAGCATGGTTTGTGCC	Plasmid construction, P_{luxO}-*mRuby3*
ME-525	CTTAATCAATTCTTCACCCTTAGATACCATAAGTAGATAACGAGACTTTTGACCTTC	Plasmid construction, P_{luxO}-*mRuby3*
ME-526	ATGGTATCTAAGGGTGAAGAATTGATTA	Plasmid construction, P_{luxO}-*mRuby3* (*mRuby3* forward)
ME-527	GCATTGAACACCATAGCACAGAGTAGTGATTATTACTTATATAATTCATCCATTCCACCC	Plasmid construction, transcriptional reporters (*mRuby3* reverse)
ME-528	TGAGACGGGCAACAGCTGATTGCCCTTCACAAGTAGATAACGAGACTTTTGACCTTC	Plasmid construction, P_{qrr1}-*mRuby3*
ME-555	CCTAGGCCTGTCGAGGCTGTTTCCTGTGTGAAAAGTATACAGCATGGTTTGTGCC	Plasmid construction, P_{qrr1}-*mRuby3*
ME-554	CACACAGGAAACAGCCTCGAC	Plasmid construction, transcriptional reporters (rbs-*mRuby3* forward)

STR-0129	CTCGGGTCACCTATCCAACTGA	qRT-PCR, *qrr*1 (*V. harveyi)*
STR-0130	TCGGATCTATTGGCTCGTTCTG	qRT-PCR, *qrr*1 (*V. harveyi)*
STR-0131	CTTAAGCCGAGGGTCACCTAGC	qRT-PCR, *qrr*2 (*V. harveyi)*
STR-0132	CAATTAGGGCGATTGGCTTATGT	qRT-PCR, *qrr*2 (*V. harveyi)*
STR-0036	CTTAAGCCGAGGGTCACCTAGC	qRT-PCR, *qrr*3 (*V. harveyi)*
STR-0037	ACAAATTCGAGTCCACTAACAACGT	qRT-PCR, *qrr*3 (*V. harveyi)*
ME-251	GTTGATTGGCGGTATATACTTGTG	qRT-PCR, *qrr*4 (*V. harveyi)*
ME-252	CCTTATTAAGCCGAGGGTCAC	qRT-PCR, *qrr*4 (*V. harveyi)*
STR-0133	GACGTTGTTAGTGAACCCAATTGTT	qRT-PCR, *qrr*5 (*V. harveyi)*
STR-0134	CACAAGGTTTGTGATTGGCTGTATA	qRT-PCR, *qrr*5 (*V. harveyi)*
ME-566	TGAGACGGGCAACAGCTGATTGCCCTTCACCG GGTGAAGTTGCGAGTTTCA	Plasmid construction, P_{qrr2}-*mRuby3*
ME-567	CCTAGGCCTGTCGAGGCTGTTTCCTGTGTGAA AAGAATTATGCATTAATCATGCCAG	Plasmid construction, P_{qrr2}-*mRuby3*
ME-568	TGAGACGGGCAACAGCTGATTGCCCTTCACGT GTGCTGATCCCAATTGTTCTTG	Plasmid construction, P_{qrr3}-*mRuby3*
ME-569	CCTAGGCCTGTCGAGGCTGTTTCCTGTGTGCA CTAAATGATGCAGTTAGTGTGCC	Plasmid construction, P_{qrr3}-*mRuby3*
ME-570	TGAGACGGGCAACAGCTGATTGCCCTTCACTG ATGAAAATCGCCGATGAACG	Plasmid construction, P_{qrr4}-*mRuby3*
ME-571	CCTAGGCCTGTCGAGGCTGTTTCCTGTGTGAT CTGTATAAAGCACGATGCGT	Plasmid construction, P_{qrr4}-*mRuby3*
ME-572	TGAGACGGGCAACAGCTGATTGCCCTTCACCT ATCGAGACCGCATTGACAG	Plasmid construction, P_{qrr5}-*mRuby3*
ME-573	CCTAGGCCTGTCGAGGCTGTTTCCTGTGTGTT ACAACTAAAGCATTAGGCATGCC	Plasmid construction, P_{qrr5}-*mRuby3*
ME-1024	CAATTGTGGTTTCTTATGAAGTCCATAC	P_{luxC} EMSA probe 1 forward primer
ME-1025	TTTAAGTGGTTGCTGCTACTAGAG	P_{luxC} EMSA probe 1 reverse primer
ME-1026	CTCTAGTAGCAGCAACCACTTAAA	P_{luxC} EMSA probe 2 forward primer
ME-1027	CACTAAAGCAACCATACTCATAAATATTG	P_{luxC} EMSA probe 2 reverse primer

ME-1028	CAATATTTATGAGTATGGTTGCTTTAGTG	P_{luxC} EMSA probe 3 forward primer
ME-1029	TTATAATTAGTCATAACATTTAACAAACAACGAA	P_{luxC} EMSA probe 3 reverse primer
ME-1030	TTCGTTGTTTGTTAAATGTTATGACTAATTATAA	P_{luxC} EMSA probe 4 forward primer
ME-1031	TTTTAACCAGATTTATTAAGCAGATCAAAC	P_{luxC} EMSA probe 4 reverse primer
ME-1032	GTTTGATCTGCTTAATAAATCTGGTTAAAA	P_{luxC} EMSA probe 5 forward primer
ME-1033	TCCATATCAAGAGCTTCTCCTTTG	P_{luxC} EMSA probe 5 reverse primer
ME-1034	CAAAGGAGAAGCTCTTGATATGGA	P_{luxC} EMSA probe 6 forward primer
ME-1035	TTCTTCAAAACTGATCTCAAATCGATT	P_{luxC} EMSA probe 6 reverse primer
ME-443	GCTTAATTACCTCCTCTTCCTTAGCTCCTGAATTCCTAG	Plasmid construction, overexpression constructs in pFED343
ME-636	CAGGAGCTAAGGAAGAGGAGGTAATTAAGCATGGACTCAATTGCAAAGAGACCT	Plasmid construction, P_{tac}-*luxR*
ME-637	AGCATTGAACACCATAGCACAGAGTAGTGATTAGTGATGTTCACGGTTGTAGATG	Plasmid construction, P_{tac}-*luxR*
ME-620	GCTTAATTACCTCCTTCAGACCGCTTCTGCGTTC	Plasmid construction, P_{BAD}-*luxT*
ME-621	AGAATTTGCCTGGCGGCAG	Plasmid construction, P_{BAD}-*luxT*
ME-622	GCAGAAGCGGTCTGAAGGAGGTAATTAAGCATGCCAAAGCGTAGTAAAGAAGATAC	Plasmid construction, P_{BAD}-*luxT*
ME-623	CCACCGCGCTACTGCCGCCAGGCAAATTCTTTATTTGCTCATTTGAATTAACGAACG	Plasmid construction, P_{BAD}-*luxT*
ME-790	TTAAGCTGCAAGGGCAAATCG	qRT-PCR, *hfq* (*E. coli)*
ME-791	GGACAACAGTAGAAATCGCGTG	qRT-PCR, *hfq* (*E. coli)*
ME-128	GAAGATCATGGATGCCGTTGTTG	qRT-PCR, *luxT* (*V. harveyi)*
ME-415	AATGGTGGCTAATACCTGTACGC	qRT-PCR, *luxT* (*V. harveyi)*
ME-398	GGGTTGAGAAGCGGTGTAAGTGAACTGCATTTGTGAGCAAGGCGTTGACTTCGTAGC	Plasmid construction, *VIBHAR_RS03920* deletion
ME-399	GGTAGGACTAGACACAAGCAACC	Plasmid construction, *VIBHAR_RS03920* deletion
ME-400	TTCATGAGGTTGCTTGTGTCTAGTCCTACCCCTGCTTAATTATATCGCCCAATAG	Plasmid construction, *VIBHAR_RS03920* deletion

ME-401	ACGCCTGAATAAGTGATAGGGCCCGATCCCTT GTGCTCAGTTTAATGCTGGTG	Plasmid construction, *VIBHAR_RS03920* deletion
STR-0383	ACATCAACTCAAATGGCAAGG	qRT-PCR, *luxR* (*V. harveyi)*
STR-0384	GCAAACACTTCAAGAGCGATTT	qRT-PCR, *luxR* (*V. harveyi)*
STR-0381	ATCCATCAACTCTAGGTGATAAACG	qRT-PCR, *aphA* (*V. harveyi)*
STR-0382	CGTCGCGAGTGCTAAGTACA	qRT-PCR, *aphA* (*V. harveyi)*
ME-778	CGGCAACCAAAAAAGTGGTCG	qRT-PCR, *VIBHAR_RS11785*
ME-779	ACCCCATTGTTGGTTGTTCATGTTG	qRT-PCR, *VIBHAR_RS11785*
ME-782	GGCTATCATGGGGAGATCAAGTC	qRT-PCR, *VIBHAR_RS11620*
ME-783	GGTGATGGGCATTGAGACGTTAC	qRT-PCR, *VIBHAR_RS11620*
LF-495	AAACTGGCGCTTGATACAGG	qRT-PCR, *VIBHAR_RS16980*
LF-496	ACATTCTGCACCACTCGTTG	qRT-PCR, *VIBHAR_RS16980*
ME-780	AGACAACAGCTCCAATACGGC	qRT-PCR, *VIBHAR_RS25670*
ME-781	ATTTGGGTTGGCTTTGGTCTCTAC	qRT-PCR, *VIBHAR_RS25670*
LF-342	GAGTCGATGCCTCAAACCAC	qRT-PCR, *VIBHAR_RS26745*
LF-343	AGGAACTTCACCGAGTGTGT	qRT-PCR, *VIBHAR_RS26745*
LF-RT27	GACAGTGAAAAGTCTGGCCC	qRT-PCR, *VIBHAR_RS24795*
LF-RT28	TGACTTGCGCTTGGAAACTT	qRT-PCR, *VIBHAR_RS24795*
LF-RT55	TTGCTCTGAATGCCGCAAAT	qRT-PCR, *VIBHAR_RS18320*
LF-RT56	TGGCGCTCTTCTGATAGGTT	qRT-PCR, *VIBHAR_RS18320*
LF-772	CAAAACTGGCGACTGTCCAA	qRT-PCR, *VIBHAR_RS24765*
LF-773	TGCTTGCCAGATTCCCCTTA	qRT-PCR, *VIBHAR_RS24765*
LF-RT43	ACCCTTCTTGCTGCTTCTCT	qRT-PCR, *VIBHAR_RS26565*

LF-RT44	ACCAACACAATGGGATGCTG	qRT-PCR, *VIBHAR_RS26565*
YS-611	ACGAAGCACAGCGTATCATC	qRT-PCR, *VIBHAR_RS21890*
YS-612	TAGCAGCTGGCTCACTTCTT	qRT-PCR, *VIBHAR_RS21890*
LF-RT13	CGACCGATTGGAAAACGCTA	qRT-PCR, *VIBHAR_RS01950*
LF-RT14	ACGGTTGGCTATAACCTGCT	qRT-PCR, *VIBHAR_RS01950*
LF-RT19	AGTCCAAAGTATCGCTGAACA	qRT-PCR, *VIBHAR_RS11480*
LF-RT20	TACGTTGAACATCAGCCCCT	qRT-PCR, *VIBHAR_RS11480*
LF-497	TTTTGCTTCAACAGGCGCTA	qRT-PCR, *VIBHAR_RS18695*
LF-498	TGTCTATCTACGCATCGGCT	qRT-PCR, *VIBHAR_RS18695*
LF-RT1	CGTGAAGTCAGTCGTTTGGT	qRT-PCR, *VIBHAR_RS27840*
LF-RT2	GCATGTTCTGGATTTTGCGT	qRT-PCR, *VIBHAR_RS27840*
ME-82	CATTGCTTACCTCGCTCTCAG	qRT-PCR, *luxMN* (*V. harveyi)*
ME-83	GTATGGCGATAAGCCACTGATTAC	qRT-PCR, *luxMN* (*V. harveyi)*
ME-1042	GGGTTGAGAAGCGGTGTAAGTGAACTGCATTG TCGCTGGTGGCAATCTTG	Plasmid construction, pRE112-*luxO* D61E Δ*qrr*1
ME-1043	CTCGAGCAGAATAAGATCAGGAATG	Plasmid construction, pRE112-*luxO* D61E Δ*qrr*1
ME-1044	CATCGCATTCCTGATCTTATTCTGCTCGAGCTT CGTCTACCTGATATGACGG	Plasmid construction, pRE112-*luxO* D61E Δ*qrr*1
ME-1045	ACGCCTGAATAAGTGATAGGGCCCGATCCCAT TGGCGCACAACAGGCTG	Plasmid construction, pRE112-*luxO* D61E Δ*qrr*1
ME-447	CAGGAGCTAAGGAAGAGGAGGTAATTAAGCAT GCCAAAGCGTAGTAAAGAAGATAC	Plasmid construction, P_{tac}-*luxT*
ME-448	AGCATTGAACACCATAGCACAGAGTAGTGATTA TTTGCTCATTTGAATTAACGAACG	Plasmid construction, P_{tac}-*luxT*
ME-981	TGAGACGGGCAACAGCTGATTGCCCTTCACAG CCCGAGCATACTAGTGATG	Plasmid construction, P_{11785}-*lux*
ME-982	GCCTGTCGAGGCTGTTTCCTGTGTGAATTAAC CTTTTATTATGGTTGTGTATTTTCTTAT	Plasmid construction, P_{11785}-*lux*
ME-1121	TAGGAATTCAATTAGGAGGTAATTAAGCATGGA AAAACACTTACCTTTAATAATAAATGG	Plasmid construction, transcriptional *lux* reporters

ME-1137	GCATTGAACACCATAGCACAGAGTAGTGATTATTACAAATAAGCGAACGCGTCC	Plasmid construction, transcriptional *lux* reporters
ME-985	TGAGACGGGCAACAGCTGATTGCCCTTCACGCTCTGGGATAACGTCATTAAGTG	Plasmid construction, P_{11620}-*lux*
ME-986	CCTAGGCCTGTCGAGGCTGTTTCCTGTGTGGTCCTTTATTTTAATGATTGAGTTGGTGC	Plasmid construction, P_{11620}-*lux*
ME-987	TGAGACGGGCAACAGCTGATTGCCCTTCACCAACATACTGGTCGACATCCCAG	Plasmid construction, P_{16980}-*lux*
ME-988	CCTAGGCCTGTCGAGGCTGTTTCCTGTGTGGTACCTAAAAGTGTAACCATAGCCAG	Plasmid construction, P_{16980}-*lux*
ME-983	TGAGACGGGCAACAGCTGATTGCCCTTCACACTAATGGAATACAACAAGATATAAGTCAC	Plasmid construction, P_{25670}-*lux*
ME-984	CCTAGGCCTGTCGAGGCTGTTTCCTGTGTGGCAACATTATTTAGCAACGCGC	Plasmid construction, P_{25670}-*lux*
ME-1006	GATTAAGCATTGGTAACTGTCAGACC	Plasmid construction, p*tetA*-Kan
ME-1007	AGTTTGTAGAAACGCAAAAAGGCC	Plasmid construction, p*tetA*-Kan
ME-1008	ACGGATGGCCTTTTTGCGTTTCTACAAACTCCTGTTAAGTATCTTCCTGGCATC	Plasmid construction, p*tetA*-Kan
ME-1009	ACTTGGTCTGACAGTTACCAATGCTTAATCCACATGGTCCTTCTTGAGTTTGTAAC	Plasmid construction, p*tetA*-Kan
ME-976	ACTAGTTCTAGAGCGGCCG	Plasmid construction, P_{tetA} *mVenus* translational reporters
ME-944	CTGTTTTGGCGGATGAGAGAAG	Plasmid construction, P_{tetA} *mVenus* translational reporters
ME-993	CACCGCGGTGGCGGCCGCTCTAGAACTAGTGCATTTTTGCTACGAATATACACACATAAG	Plasmid construction, P_{tetA}-*11785'-'mVenus*
ME-785	AACTCCAGTGAAAAGTTCTTCTCCTTTACTGACCAGCGATAATAAAGTGACGTTTC	Plasmid construction, P_{tetA}-*11785'-'mVenus*
ME-640	AGTAAAGGAGAAGAACTTTTCACTGG	Plasmid construction, P_{tetA} *mVenus* translational reporters
ME-994	GAAAATCTTCTCTCATCCGCCAAAACAGTTATTATTTGTATAGTTCATCCATGCCATGTG	Plasmid construction, P_{tetA} *mVenus* translational reporters
ME-998	CACCGCGGTGGCGGCCGCTCTAGAACTAGTGAGTACGCCCGCTTTTAGGTCAAAA	Plasmid construction, P_{tetA}-*11620'-'mVenus*
ME-789	AACTCCAGTGAAAAGTTCTTCTCCTTTACTCGTCGATAAGAAAGAAAGTGCAAGC	Plasmid construction, P_{tetA}-*11620'-'mVenus*
ME-999	CACCGCGGTGGCGGCCGCTCTAGAACTAGTCAACCGGTTGCATTGTTCGTGAA	Plasmid construction, P_{tetA}-*16980'-'mVenus*
ME-990	AACTCCAGTGAAAAGTTCTTCTCCTTTACTCGCAGTACCTAAAAGTGTAACCATA	Plasmid construction, P_{tetA}-*16980'-'mVenus*
ME-997	CACCGCGGTGGCGGCCGCTCTAGAACTAGTATGCCCAATTAAATTATGGCGCGTT	Plasmid construction, P_{tetA}-*25670'-'mVenus*

ME-787	AACTCCAGTGAAAAGTTCTTCTCCTTTACTACT ACCTAGCTTTGTATAGTTGAAA	Plasmid construction, P_{tetA}-*25670'-'mVenus*
ME-1063	CTTCCTTAGCTCCTGAATTCCTAG	Plasmid construction, P_{tac}-*qrr*1
ME-1064	ACAGGCCTAGGAATTCAGGAGCTAAGGAAGGG ACCCCTCGGGTCACCTATC	Plasmid construction, P_{tac}-*qrr*1
ME-1065	AGCATTGAACACCATAGCACAGAGTAGTGACG AACAGTTAATTCTTCTCTAACCG	Plasmid construction, P_{tac}-*qrr*1
ME-624	GGGTTGAGAAGCGGTGTAAGTGAACTGCATTG TGTGAAACCCGCGATAAGC	Plasmid construction, *V. cholerae luxT* deletion
ME-625	CATGGTCAGGCTCTTTTCTAACG	Plasmid construction, *V. cholerae luxT* deletion
ME-626	GATTTGACGTTAGAAAAGAGCCTGACCATGAAT TGATTCTTCACCTTCTGCCTAC	Plasmid construction, *V. cholerae luxT* deletion
ME-627	ACGCCTGAATAAGTGATAGGGCCCGATCCC ATGCTCACCCTTGCCGATATG	Plasmid construction, *V. cholerae luxT* deletion
ME-903	GGGTTGAGAAGCGGTGTAAGTGAACTGCATCG CGCTATTGTCTGGTTCAG	Plasmid construction, *V. parahaemolyticus swrT* deletion
ME-904	CTTTGGCATACTTTAAGCTCTTCTC	Plasmid construction, *V. parahaemolyticus swrT* deletion
ME-905	ACAAAGAGAAGAGCTTAAAGTATGCCAAAGTG GTTGATTGGACGCTCGC	Plasmid construction, *V. parahaemolyticus swrT* deletion
ME-906	ACGCCTGAATAAGTGATAGGGCCCGATCCCGG AATCGTAACTGCGCTCATC	Plasmid construction, *V. parahaemolyticus swrT* deletion
ME-969	GGGTTGAGAAGCGGTGTAAGTGAACTGCATGC TTAGGTGAGTTCGATGTCTTAG	Plasmid construction, pRE112-*luxO* D61E (*V. parahaemolyticus)*
ME-970	CTCGAGAAGAATAAGATCTGAAATTCGGTG	Plasmid construction, pRE112-*luxO* D61E (*V. parahaemolyticus)*
ME-971	CACCGAATTTCAGATCTTATTCTTCTCGAGCTT CGTCTGCCTGATATGACG	Plasmid construction, pRE112-*luxO* D61E (*V. parahaemolyticus)*
ME-972	ACGCCTGAATAAGTGATAGGGCCCGATCCCGC GGCGGTGGCAACATATC	Plasmid construction, pRE112-*luxO* D61E (*V. parahaemolyticus)*
ME-1054	TGAGACGGGCAACAGCTGATTGCCCTTCACCC TCAACCATCAAAAGGTAACGAG	Plasmid construction, P_{qrr1}-*mRuby3* (*V. parahaemolyticus*)
ME-1055	CCTAGGCCTGTCGAGGCTGTTTCCTGTGTGCT AATATATCAGCATGCTTTATGCCA	Plasmid construction, P_{qrr1}-*mRuby3* (*V. parahaemolyticus*)
ME-962	GGGTTGAGAAGCGGTGTAAGTGAACTGCATTG AGCGTGTCGAAATTATACGTG	Plasmid construction, pRE112-*luxO* D55E (*A. fischeri*)
ME-963	CTCTAGTAACACAAGATCAGGGGTTC	Plasmid construction, pRE112-*luxO* D55E (*A. fischeri*)
ME-964	TTAAGAACCCCTGATCTTGTGTTACTAGAGTTG CGCCTGCCTGACATG	Plasmid construction, pRE112-*luxO* D55E (*A. fischeri*)
ME-965	ACGCCTGAATAAGTGATAGGGCCCGATCCCGG CAGCATGGATAATTCGACTTC	Plasmid construction, pRE112-*luxO* D55E (*A. fischeri*)

ME-1052	TGAGACGGGCAACAGCTGATTGCCCTTCACGC AGCAACGGAAGCAGTATC	Plasmid construction, P_{qrr1}-*mRuby3* (*A. fischeri*)
ME-1053	CCTAGGCCTGTCGAGGCTGTTTCCTGTGTGAT ATACCTATTGCAGGGAGCGTG	Plasmid construction, P_{qrr1}-*mRuby3* (*A. fischeri*)
ME-949	GGGTTGAGAAGCGGTGTAAGTGAACTGCATGG TGCTATGTATAAGGGTGACCG	Plasmid construction, pRE112-*luxO* D55E Δ*qrr*1 (*A. fischeri)*
ME-950	TCTGCTATAAAATCAATAACTAACTATTCAC	Plasmid construction, pRE112-*luxO* D55E Δ*qrr*1 (*A. fischeri)*
ME-951	TGAATAGTTAGTTATTGATTTTATAGCAGAATAT ACCTATTGCAGGGAGCGTG	Plasmid construction, pRE112-*luxO* D55E Δ*qrr*1 (*A. fischeri)*
ME-952	ACGCCTGAATAAGTGATAGGGCCCGATCCCCT AGCCAAGGGTCTCGGTTTG	Plasmid construction, pRE112-*luxO* D55E Δ*qrr*1 (*A. fischeri)*
ME-93	GTTAACGGGATCAAACTACAGGGAC	qRT-PCR, *hfq* (*A. fischeri)*
ME-94	AGTAGAAATCGCATGCTTGTATACC	qRT-PCR, *hfq* (*A. fischeri)*
ME-1090	AACAAGGCTATCTCCAGAAAAGC	qRT-PCR, *litR* (*A. fischeri)*
ME-1091	TCTGCAATATCAGCATGACCACC	qRT-PCR, *litR* (*A. fischeri)*

S3 Table. Plasmids used in this study

Plasmid Name	Stock Name	Description	Origin, marker	Reference
pET15b	pET15b	Overexpression vector for protein purification	pBR322, Amp^R	Novagen
pET15b-*luxT-6xHis*	pME127	*luxT-6xHis* overexpression vector for protein purification, cloned in pET15b	pBR322, Amp^R	This study
pRE112	pRE112	allelic exchange vector harboring *sacB* as a counter-selectable marker	R6Kγ, Cam^R	[1]
pRE112-Δ*luxT*	pME12	*V. harveyi luxT* deletion construct in pRE112	R6Kγ, Cam^R	This study
pRE112-*aphA-3xFLAG*	pME146	*V. harveyi aphA-3xFLAG* allele exchange construct in pRE112	R6Kγ, Cam^R	This study
pRE112-*3xFLAG-luxR*	pME147	*V. harveyi 3xFLAG-luxR* allele exchange construct in pRE112	R6Kγ, Cam^R	This study
pFED343	pFED343	P_{tac} overexpression vector	P15A, Cam^R	[2]
P_{qrr1}-*mRuby3*	pME98	*V. harveyi qrr*1-*mRuby3* transcriptional reporter in pFED343 (excluding the P_{tac} promoter)	P15A, Cam^R	This study
P_{luxO}-*mRuby3*	pME96	*V. harveyi luxO-mRuby3* transcriptional reporter in pFED343 (excluding the P_{tac} promoter)	P15A, Cam^R	This study
P_{qrr2}-*mRuby3*	pME100	*V. harveyi qrr*2-*mRuby3* transcriptional reporter in pFED343 (excluding the P_{tac} promoter)	P15A, Cam^R	This study
P_{qrr3}-*mRuby3*	pME102	*V. harveyi qrr*3-*mRuby3* transcriptional reporter in pFED343 (excluding the P_{tac} promoter)	P15A, Cam^R	This study
P_{qrr4}-*mRuby3*	pME103	*V. harveyi qrr*4-*mRuby3* transcriptional reporter in pFED343 (excluding the P_{tac} promoter)	P15A, Cam^R	This study
P_{qrr5}-*mRuby3*	pME105	*V. harveyi qrr*5-*mRuby3* transcriptional reporter in pFED343 (excluding the P_{tac} promoter)	P15A, Cam^R	This study
p*luxCDABE*	pBB1	*V. harveyi luxCDABE* cloned in pLAFR (expressed from its native promoter)	oriV Tet^R	[3]
p*luxR*	pME125	*V. harveyi luxR* overexpression vector, cloned in pFED343	P15A, Cam^R	This study
pKP8-35	pKP8-35	P_{BAD} overexpression vector	pBR322, Amp^R	[4]

p*luxT*	pME109	*V. harveyi luxT* overexpression vector, cloned in pKP8-35	pBR322, Amp^R	This study
pRE112-Δ*VIBHAR_RS03920*	pME64	*V. harveyi VIBHAR_RS03920* deletion construct in pRE112	R6Kγ, Cam^R	This study
pRE112-*luxO* D61E Δ*qrr*1	pME148	*V. harveyi luxO* D61E Δ*qrr*1 allele exchange construct in pRE112	R6Kγ, Cam^R	This study
p*luxT*	pME69	*V. harveyi luxT* overexpression vector, cloned in pFED343	P15A, Cam^R	This study
P_{11785}-*lux*	pME188	*VIBHAR_RS11785-luxCDABE* transcriptional reporter in pFED343 (excluding the P_{tac} promoter)	P15A, Cam^R	This study
P_{11620}-*lux*	pME189	*VIBHAR_RS11620-luxCDABE* transcriptional reporter in pFED343 (excluding the P_{tac} promoter)	P15A, Cam^R	This study
P_{16980}-*lux*	pME190	*VIBHAR_RS16980-luxCDABE* transcriptional reporter in pFED343 (excluding the P_{tac} promoter)	P15A, Cam^R	This study
P_{25670}-*lux*	pME191	*VIBHAR_RS25670-luxCDABE* transcriptional reporter in pFED343 (excluding the P_{tac} promoter)	P15A, Cam^R	This study
pXB300	pXB300	P_{tetA} overexpression vector	pBR322, Amp^R	[5]
p*tetA*-Kan	pME149	P_{tetA} overexpression vector (Amp^R replaced with Kan^R in pXB300)	pBR322, Kan^R	This study
P_{tetA}-*11785'-'mVenus*	pME150	*VIBHAR_RS11785* translational *mVenus* reporter, expressed from the *tetA* promoter	pBR322, Kan^R	This study
P_{tetA}-*11620'-'mVenus*	pME151	*VIBHAR_RS11620* translational *mVenus* reporter, expressed from the *tetA* promoter	pBR322, Kan^R	This study
P_{tetA}-*16980'-'mVenus*	pME152	*VIBHAR_RS16980* translational *mVenus* reporter, expressed from the *tetA* promoter	pBR322, Kan^R	This study
P_{tetA}-*25670'-'mVenus*	pME153	*VIBHAR_RS25670* translational *mVenus* reporter, expressed from the *tetA* promoter	pBR322, Kan^R	This study
p*qrr*1	pME154	*V. harveyi qrr*1 overexpression vector, cloned in pFED343	P15A, Cam^R	This study
pRE112-Δ*luxT* (*V. cholerae)*	pME112	*V. cholerae luxT* deletion construct in pRE112	R6Kγ, Cam^R	This study
P_{qrr1}-*luxCDABE*	pBK1001	*qrr*1-*luxCDABE* promoter fusion	Cam^R	[6]
pRE112-Δ*swrT* (*V. parahaemolyticus)*	pME155	*V. parahaemolyticus swrT* deletion construct in pRE112	R6Kγ, Cam^R	This study

pRE112-*luxO* D61E (*V. parahaemolyticus)*	pME156	*V. parahaemolyticus luxO* D61E allele exchange construct in pRE112	R6Kγ, Cam^R	This study
P_{qrr1}-*mRuby3* (*V. parahaemolyticus*)	pME157	*V. parahaemolyticus qrr*1-*mRuby3* transcriptional reporter in pFED343 (excluding the P_{tac} promoter)	P15A, Cam^R	This study
pRE112-*luxO* D55E (*A. fischeri)*	pME158	*A. fischeri luxO* D55E allele exchange construct in pRE112	R6Kγ, Cam^R	This study
P_{qrr1}-*mRuby3* (*A. fischeri*)	pME159	*A. fischeri qrr*1-*mRuby3* transcriptional reporter in pFED343 (excluding the P_{tac} promoter)	P15A, Cam^R	This study
pRE112-*luxO* D55E Δ*qrr*1 (*A. fischeri)*	pME160	*A. fischeri luxO* D55E Δ*qrr*1 allele exchange construct in pRE112	P15A, Cam^R	This study

Table S3 References

1. Edwards RA, Keller LH, Schifferli DM. Improved allelic exchange vectors and their use to analyze 987P fimbria gene expression. Gene. 1998 Jan 30;207(2):149–57.

2. Swem LR, Swem DL, Wingreen NS, Bassler BL. Deducing receptor signaling parameters from in vivo analysis: LuxN/AI-1 quorum sensing in *Vibrio harveyi*. Cell. 2008 Aug 8;134(3):461–73.

3. Miller MB, Skorupski K, Lenz DH, Taylor RK, Bassler BL. Parallel quorum sensing systems converge to regulate virulence in *Vibrio cholerae*. Cell. 2002 Aug 9;110(3):303–14.

4. Papenfort K, Pfeiffer V, Mika F, Lucchini S, Hinton JCD, Vogel J. SigmaE-dependent small RNAs of Salmonella respond to membrane stress by accelerating global *omp* mRNA decay. Mol Microbiol. 2006 Dec;62(6):1674–88.

5. Bina XR, Wong EA, Bina TF, Bina JE. Construction of a tetracycline inducible expression vector and characterization of its use in *Vibrio cholerae*. Plasmid. 2014 Nov;76:87–94.

6. Svenningsen SL, Waters CM, Bassler BL. A negative feedback loop involving small RNAs accelerates *Vibrio cholerae's* transition out of quorum-sensing mode. Genes Dev. 2008 Jan 15;22(2):226–38.

S1 Fig

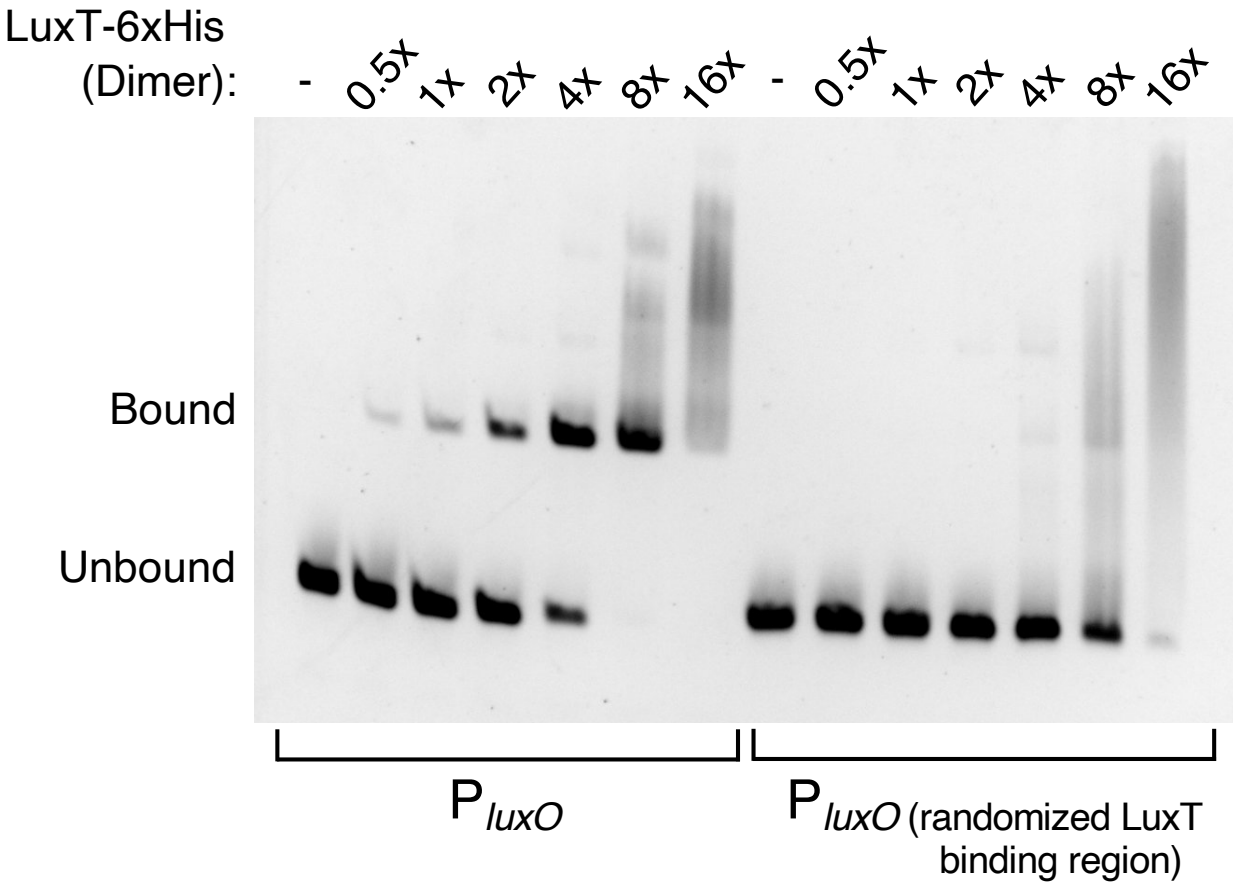
LuxT-6xHis
(Dimer):
-
0.5x
1x
2x
4x
8x
16x
-
0.5x
1x
2x
4x
8x
16x
Bound
Unbound
P luxO
P luxO (randomized LuxT binding region)

S2 Fig


luxO
START
LuxO
-102 Binding Site
5’-CATAGCCTAGCCGATTTTTCGTTGTGTTTTAAATAATAATCGCATTACGCTTTGCATTTT-3’
3’-GTATCGGATCGGCTAAAAAGCAACACAAAATTTATTATTAGCGTAATGCGAAACGTAAAA-5’
-90
-76
LuxT Binding Site
5’-GCAAATAATCATTTGTTAGACTGTGGGTATTCTAAACAAAGTAAACCGAATATCAACAGG-3’
3’-CGTTTATTAGTAAACAATCTGACACCCATAAGATTTGTTTCATTTGGCTTATAGTTGTCC-5’
-27 -24 σ54 Binding Site -12
+1
qrr1
5’-TTAAATTATGGCACAAACCATGCTGTATACTTTTGGACCCCTCGGGTCACCTATCCAACT-3’
3’-AATTTAATACCGTGTTTGGTACGACATATGAAAACCTGGGGAGCCCAGTGGATAGGTTGA-5’
5’-GACGTTGTTAGTGAACGACATGTTCACAGAACGAGCCAATAGATCCGACTGCCTATTGGC-3’
3’-CTGCAACAATCACTTGCTGTACAAGTGTCTTGCTCGGTTATCTAGGCTGACGGATAACCG-5’
5’-TTCTTTTTT-3’
3’-AAGAAAAAA-5’

S3 Fig

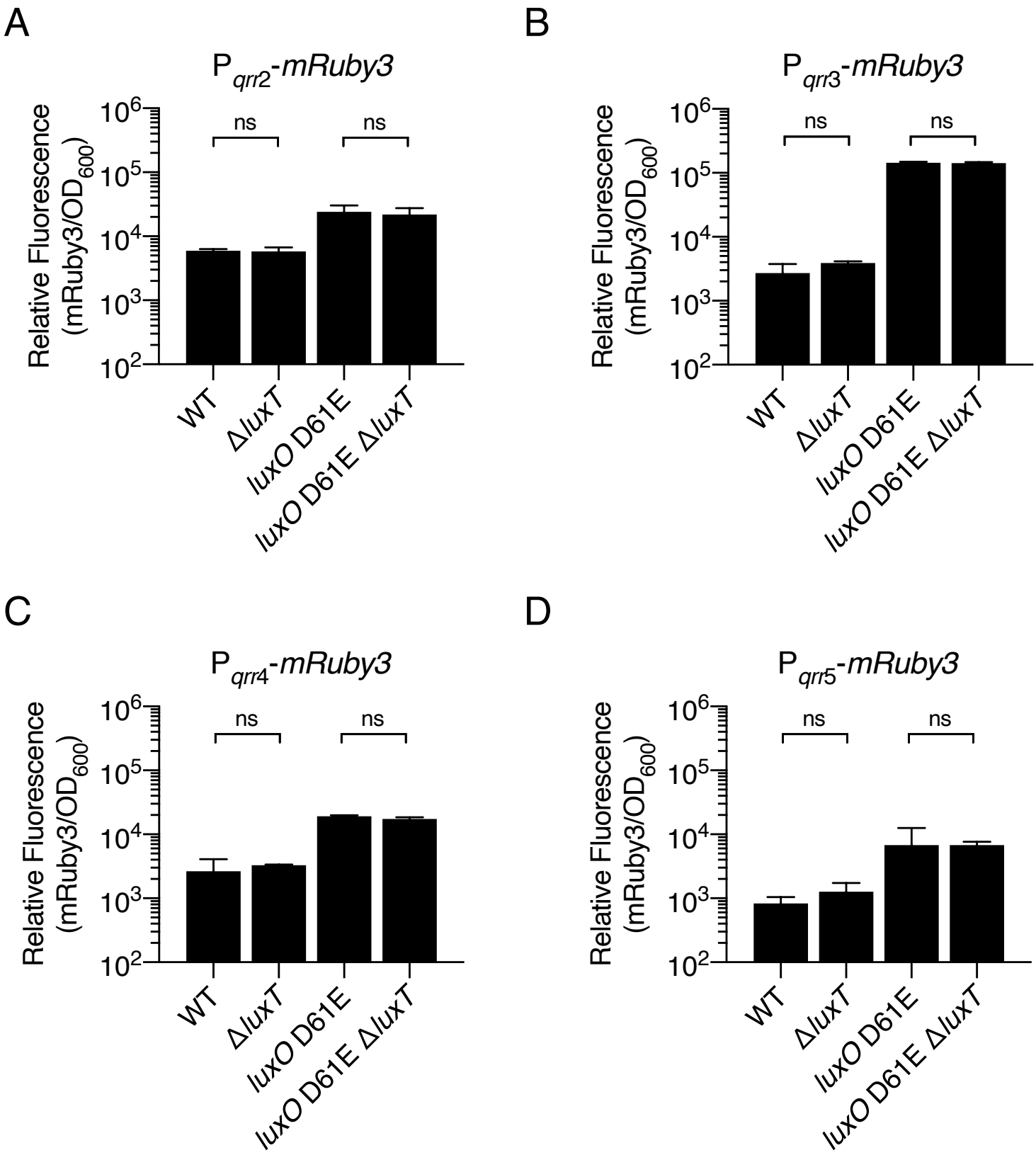
A
B
C
D
P qrr2-mRuby3
P qrr3-mRuby3
P qrr4-mRuby3
P qrr5-mRuby3
Relative Fluorescence (mRuby3/OD600)
ns
WT
ΔluxT
luxO D61E
luxO D61E ΔluxT

S4 Fig

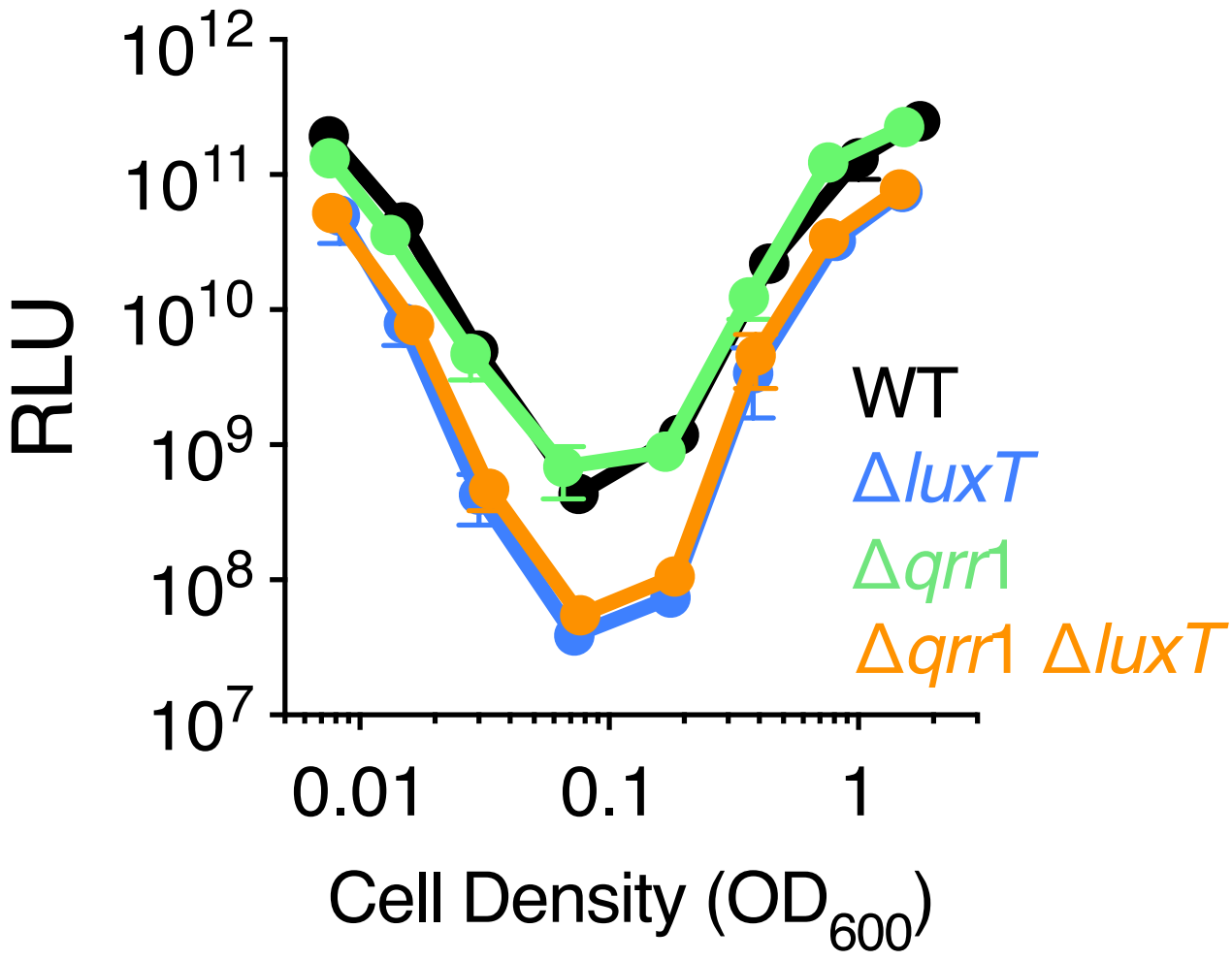
RLU
10^{12}
10^{11}
10^{10}
10^{9}
10^{8}
10^{7}
0.01
0.1
1
Cell Density (OD_{600})
WT
Δ*luxT*
Δ*qrr*1
Δ*qrr*1 Δ*luxT*

S5 Fig

A

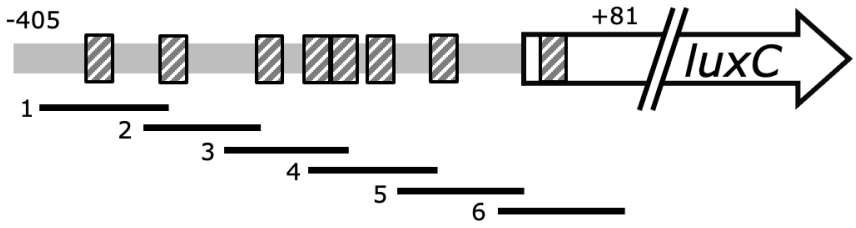
-405
+81
luxC
1
2
3
4
5
6

B

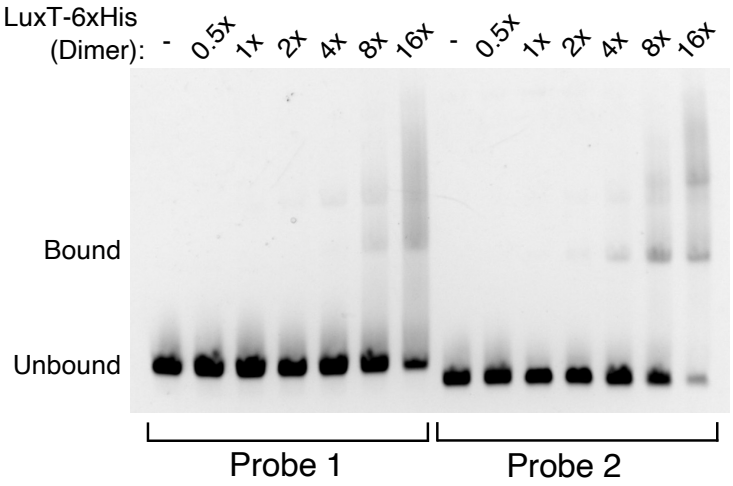
LuxT-6xHis
(Dimer):
- 0.5x 1x 2x 4x 8x 16x - 0.5x 1x 2x 4x 8x 16x
Bound
Unbound
Probe 1
Probe 2

C

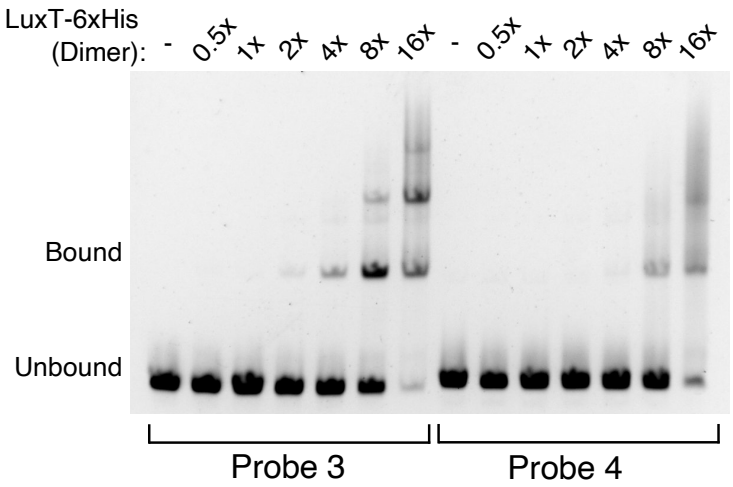
LuxT-6xHis
(Dimer):
- 0.5x 1x 2x 4x 8x 16x - 0.5x 1x 2x 4x 8x 16x
Bound
Unbound
Probe 3
Probe 4

D

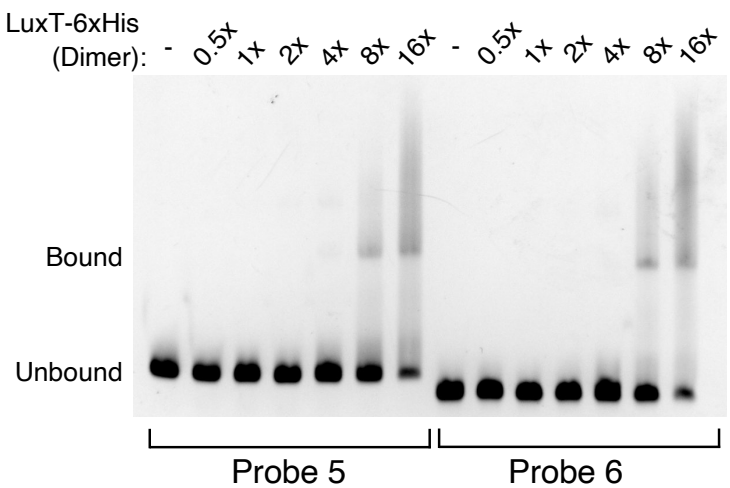
LuxT-6xHis
(Dimer):
- 0.5x 1x 2x 4x 8x 16x - 0.5x 1x 2x 4x 8x 16x
Bound
Unbound
Probe 5
Probe 6

S6 Fig

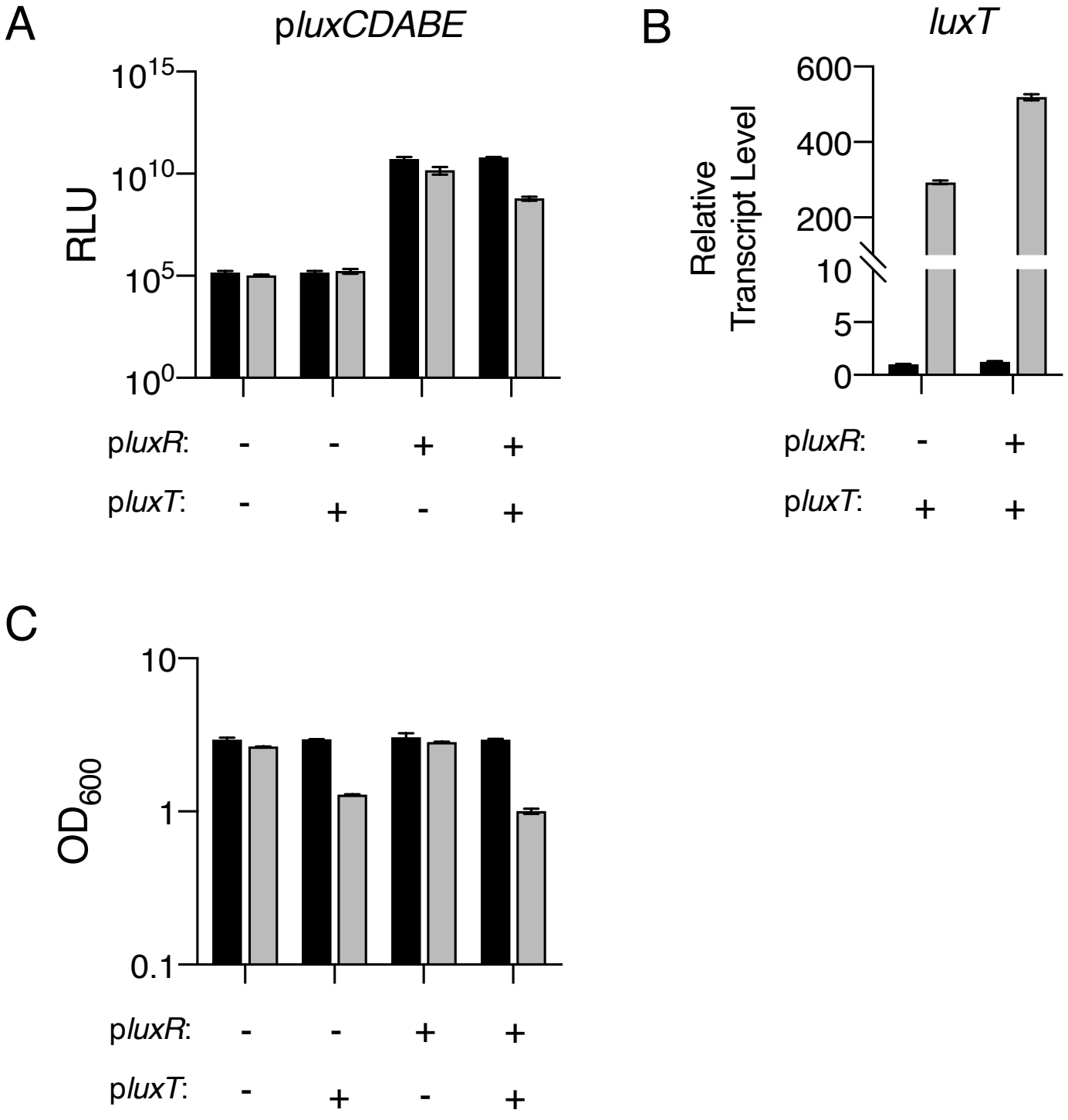
A
p*luxCDABE*
RLU
10^{15}
10^{10}
10^{5}
10^{0}
p*luxR*: - - + +
p*luxT*: - + - +
B
luxT
Relative Transcript Level
600
400
200
10
5
0
p*luxR*: - +
p*luxT*: + +
C
OD_{600}
10
1
0.1
p*luxR*: - - + +
p*luxT*: - + - +

S7 Fig

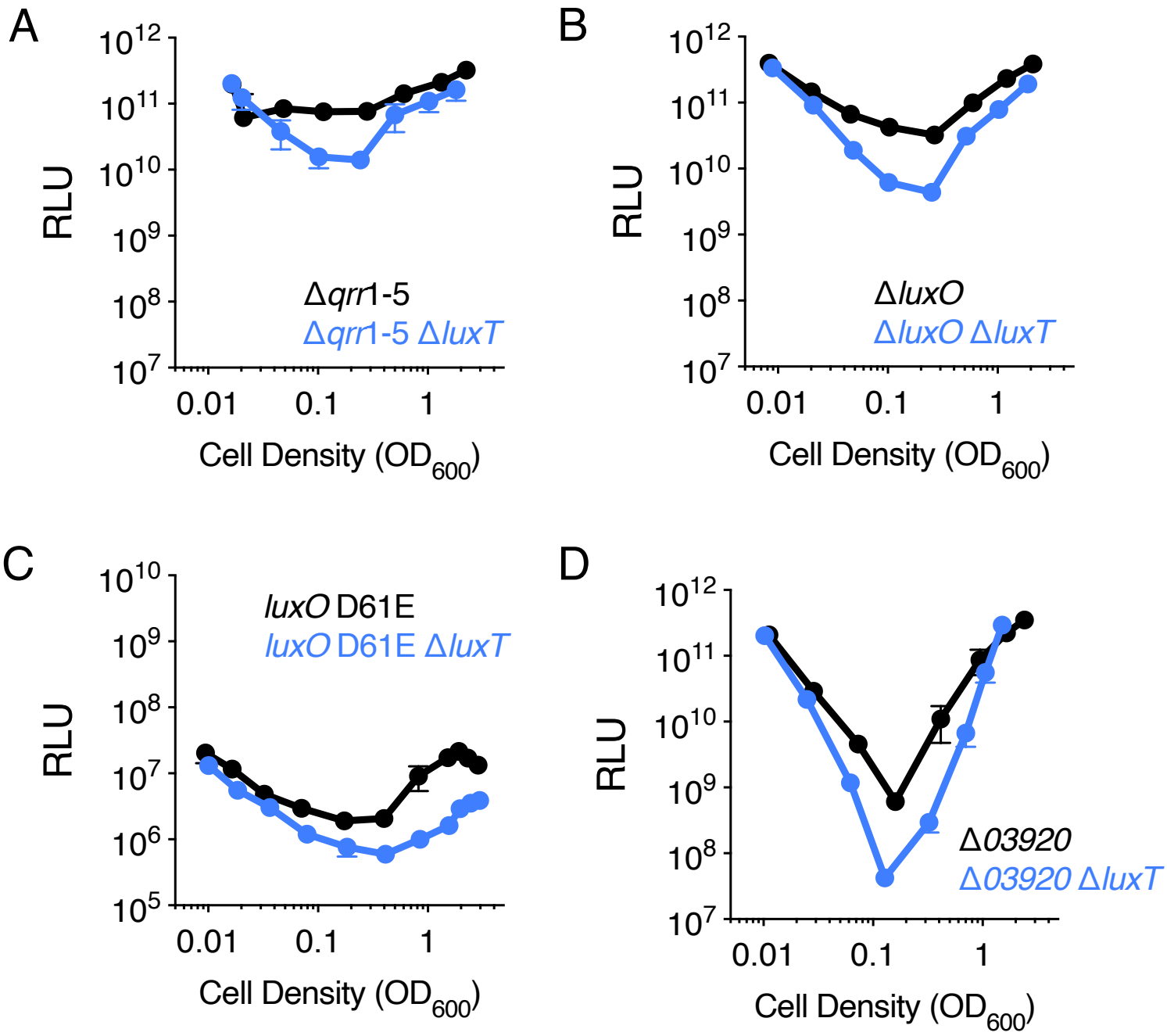
A
B
C
D
RLU
Cell Density (OD600)
0.01
0.1
1
Δqrr1-5
Δqrr1-5 ΔluxT
ΔluxO
ΔluxO ΔluxT
luxO D61E
luxO D61E ΔluxT
Δ03920
Δ03920 ΔluxT

S8 Fig

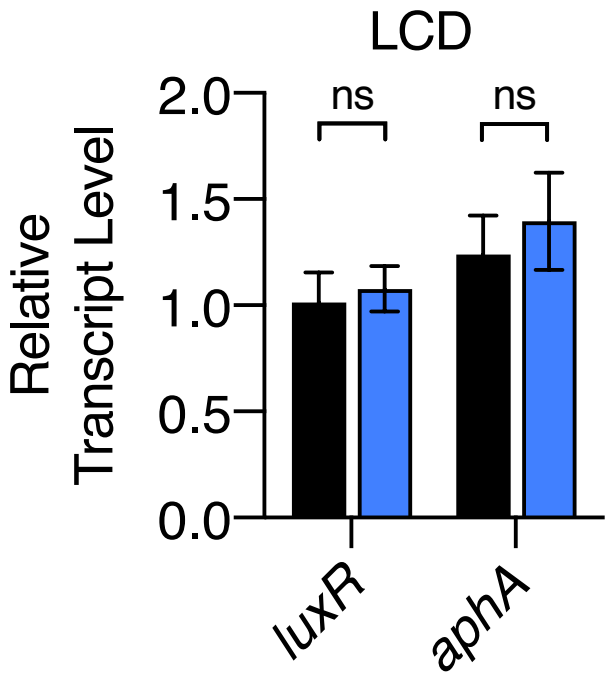

S9 Fig

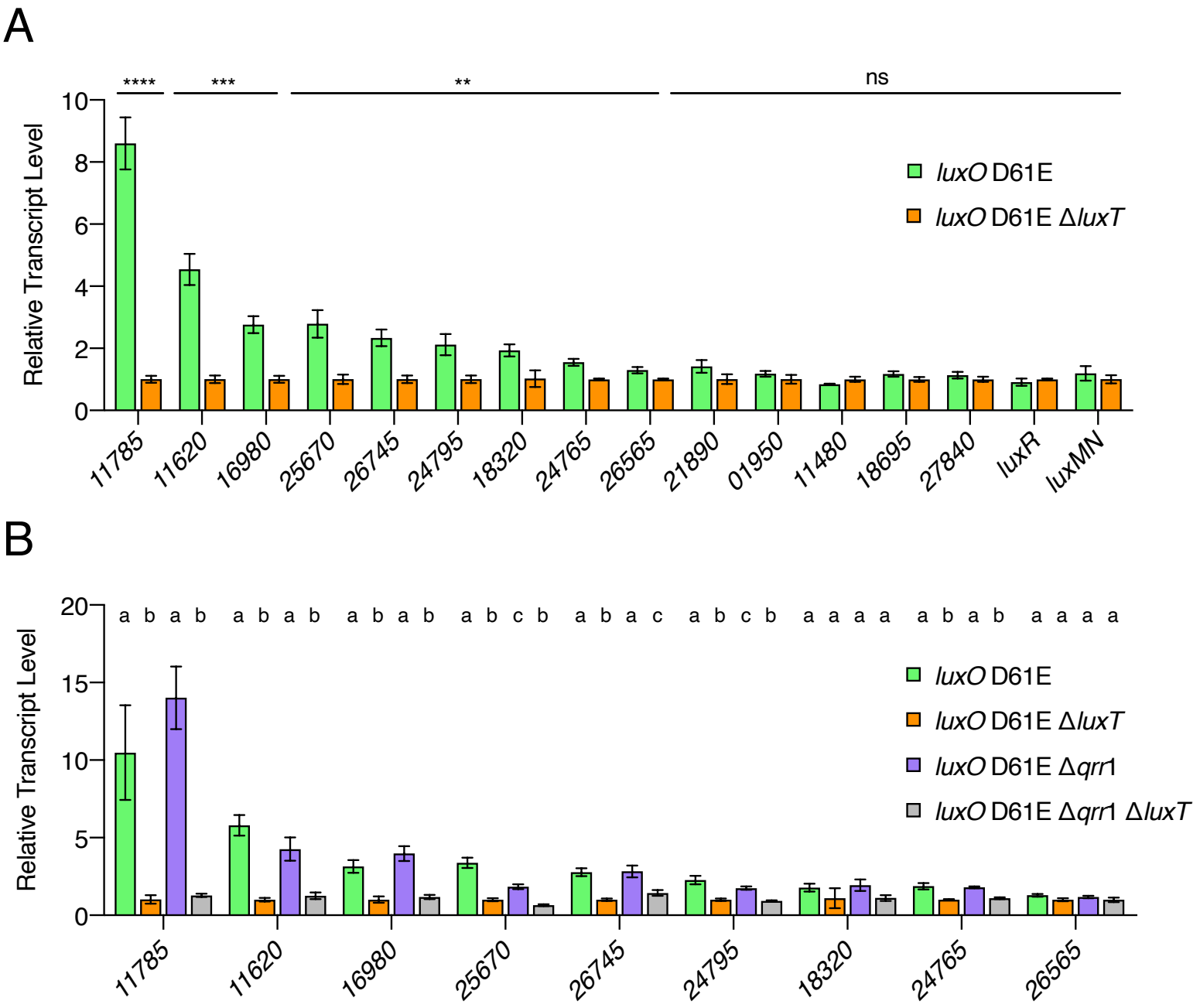
A
****
***
**
ns
Relative Transcript Level
10
8
6
4
2
0
luxO D61E
luxO D61E ΔluxT
11785
11620
16980
25670
26745
24795
18320
24765
26565
21890
01950
11480
18695
27840
luxR
luxMN
B
a b a b a b a b a b a b a b a b c b a b a c a b c b a a a a a b a b a a a a
Relative Transcript Level
20
15
10
5
0
luxO D61E
luxO D61E ΔluxT
luxO D61E Δqrr1
luxO D61E Δqrr1 ΔluxT
11785
11620
16980
25670
26745
24795
18320
24765
26565

S10 Fig

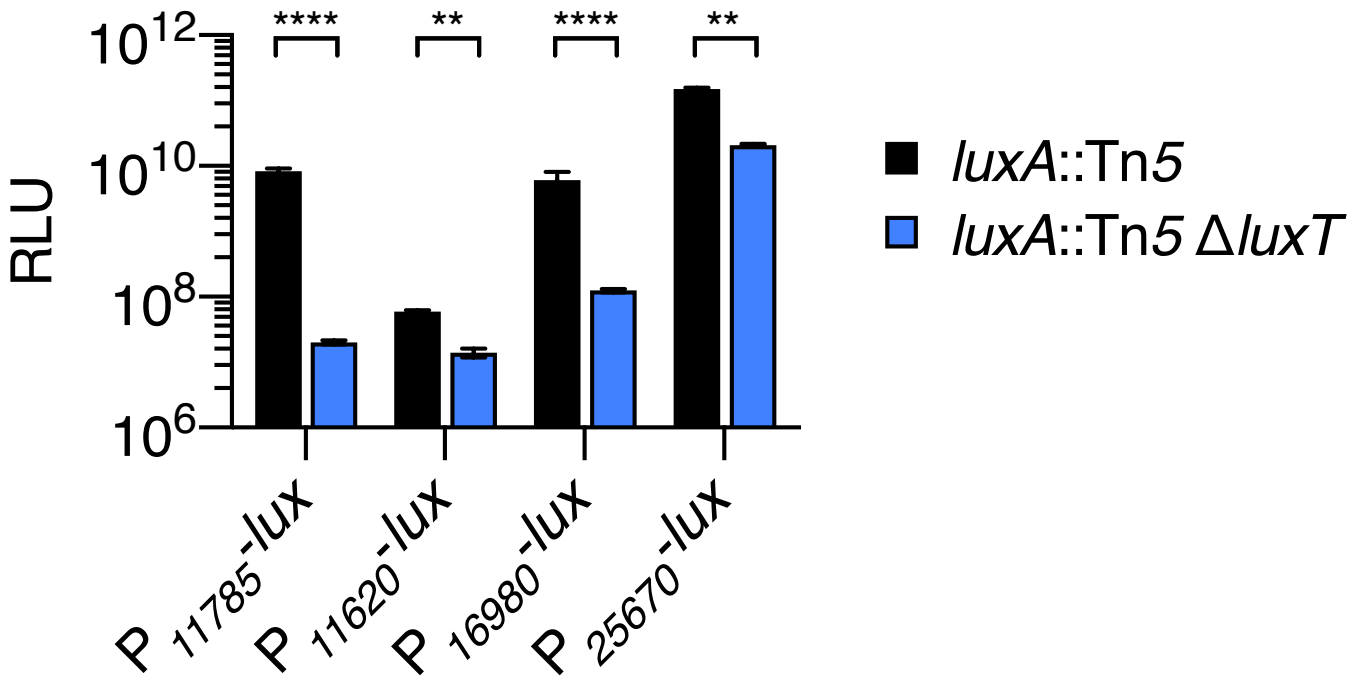
RLU
10^{12}
10^{10}
10^{8}
10^{6}
****
**
****
**
P 11785-lux
P 11620-lux
P 16980-lux
P 25670-lux
luxA::Tn5
luxA::Tn5 ΔluxT

S11 Fig

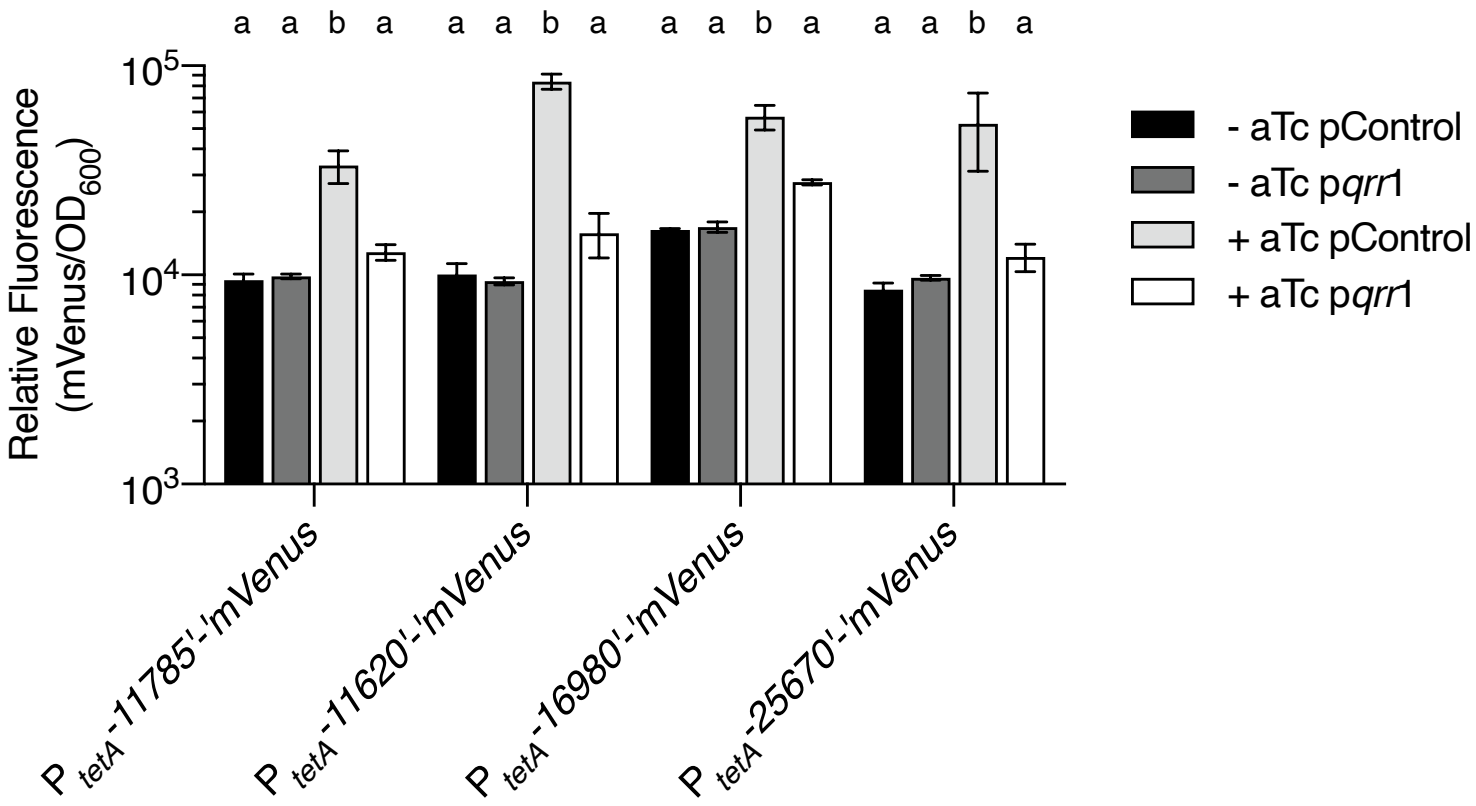
a a b a a a b a a a b a a a b a
Relative Fluorescence (mVenus/OD600)
10^5
10^4
10^3
- aTc pControl
- aTc pqrr1
+ aTc pControl
+ aTc pqrr1
P tetA-11785'-'mVenus
P tetA-11620'-'mVenus
P tetA-16980'-'mVenus
P tetA-25670'-'mVenus

S12 Fig

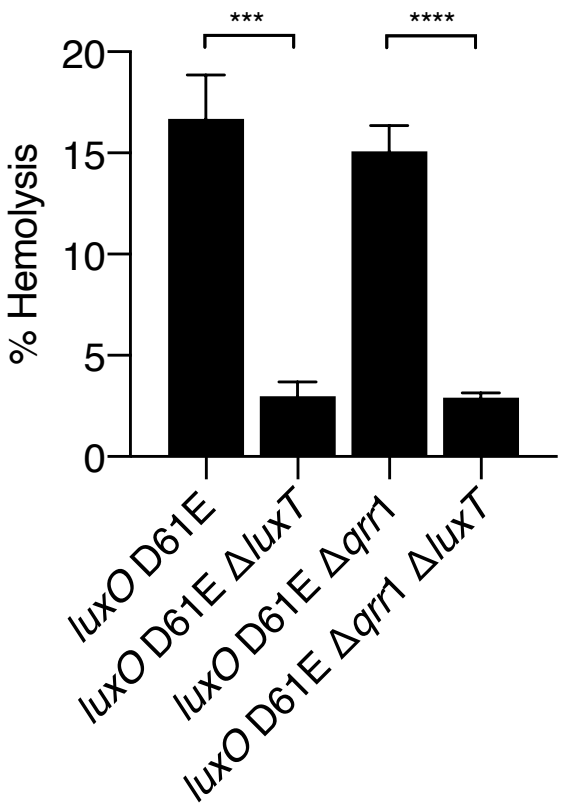
***
****
20
15
10
5
0
% Hemolysis
luxO D61E
luxO D61E ΔluxT
luxO D61E Δqrr1
luxO D61E Δqrr1 ΔluxT

S13 Fig

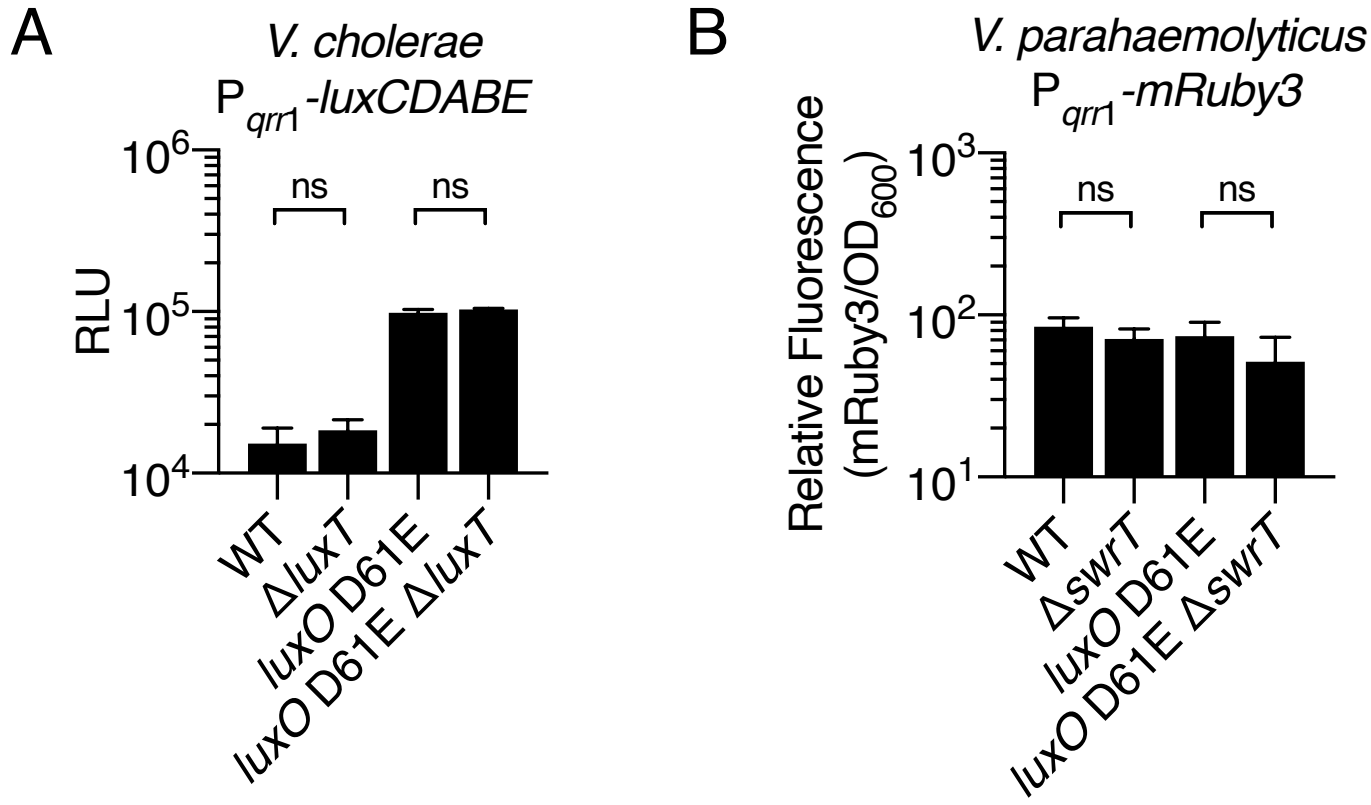
A
V. cholerae
P qrr1 -luxCDABE
RLU
10^6
10^5
10^4
ns
ns
WT
ΔluxT
luxO D61E
luxO D61E ΔluxT
B
V. parahaemolyticus
P qrr1 -mRuby3
Relative Fluorescence
(mRuby3/OD600)
10^3
10^2
10^1
ns
ns
WT
ΔswrT
luxO D61E
luxO D61E ΔswrT